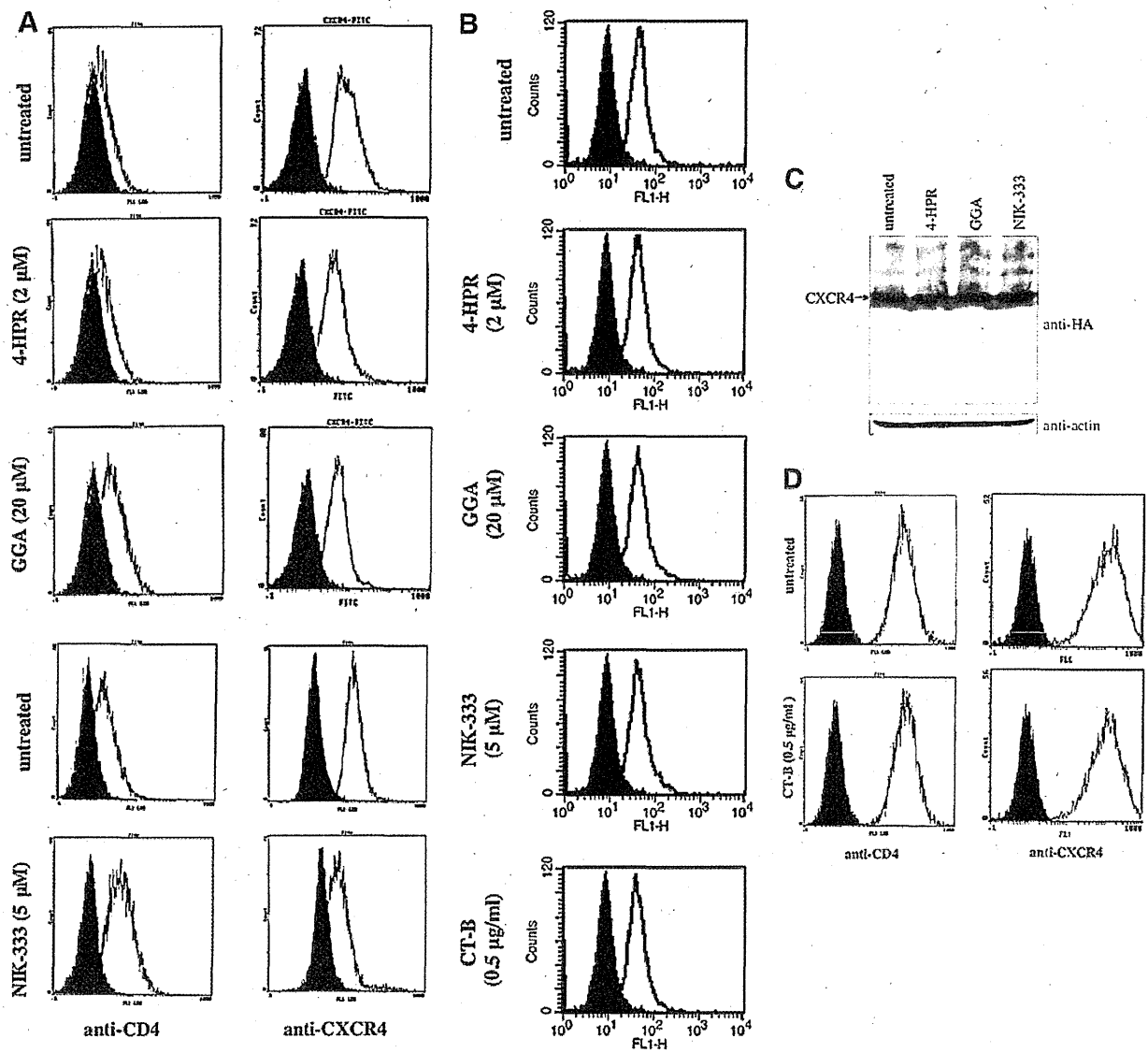

FIG. 4. Retinoid analogs inhibit cell surface expression of CXCR4. Cell surface expression of CD4 and CXCR4 in retinoid analog-treated HeLa/CD4 cells **(A)**, CCR5 in retinoid analog- or CT-B-treated NP2/CD4/R5 cells **(B)**, and CD4 and CXCR4 in CT-B-treated TE671/CD4 cells **(D)** were analyzed by flow cytometry. Closed and open areas indicate untreated cells stained with control serum or with anti-CD4, -CXCR4, or -CCR5 antibody, respectively. Representative results are shown. Expression of C-terminally HA-tagged CXCR4 was analyzed by Western immunoblotting using an anti-HA antibody **(C)**. As a control, actin expression was also analyzed.

Discussion

HAART has dramatically reduced the mortality and morbidity of HIV-1-infected patients in developed countries. However, due to the high cost of HAART, this therapy is limited in developing countries. In addition, HIV-1 variants that are resistant to HAART have emerged. Therefore, development of novel low-cost drugs that inhibit HIV-1 replication is essential.

In this study, we found that the acyclic retinoid analogs, GGA and NIK-333, suppress CXCR4-tropic HIV-1 vector infection similarly to 4-HPR.[23] Additionally, retinoids repress expression of the HIV-1 promoter,[38–40] suggesting that retinoid analogs are possible candidates for a novel anti-HIV-1 therapy. Many reports indicate that vitamin A (retinol) supplementation reduces the mortality of HIV-1-infected patients.[41–44] NIK333, a synthetic acyclic retinoid, is orally effective against liver cancer without severe side effects.[28] GGA also suppresses HIV-1 vector infection and is present in medicinal herbs. These results suggest that oral intake of a natural acyclic retinoid analog may be novel low-cost therapy against AIDS.

We also found that CT-B efficiently suppresses CXCR4-tropic HIV-1 vector infection. Gauthier and Tremblay have shown that CT-B does not inhibit HIV-1 infection, although the concentration of CT-B (10 ng/ml) used in their study was

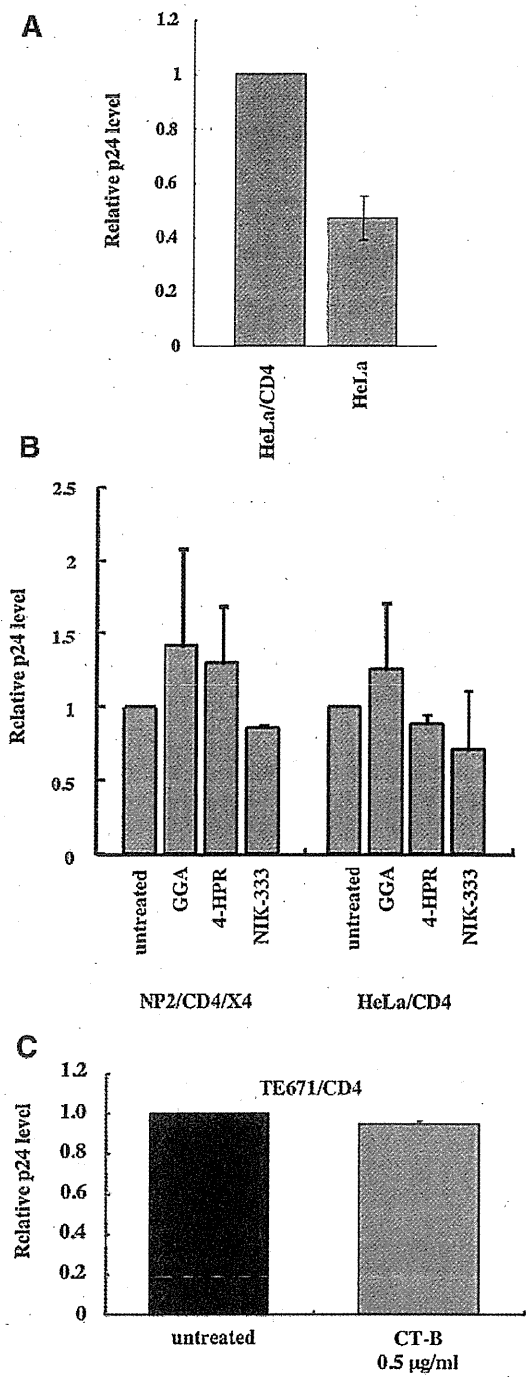

FIG. 5. Retinoid analogs and CT-B do not affect HIV-1 vector particle binding to target cells. HeLa/CD4 and HeLa cells were incubated with the HXB2 Env-containing HIV-1 vector particles at 4°C for 1h and then washed with phosphate buffered saline (PBS) **(A)**. HIV-1 particles bound to the target cells were measured by p24 ELISA. The p24 levels in untreated HeLa/CD4 cells were set to 1. HIV-1 vector particles bound to the retinoid analog-treated NP2/CD4/X4 or HeLa/CD4 cells **(B)** or to CT-B-treated TE671/CD4 cells **(C)** were measured. The p24 levels in untreated cells were set to 1. These experiments were repeated in triplicate, and results are shown as the mean+SD.

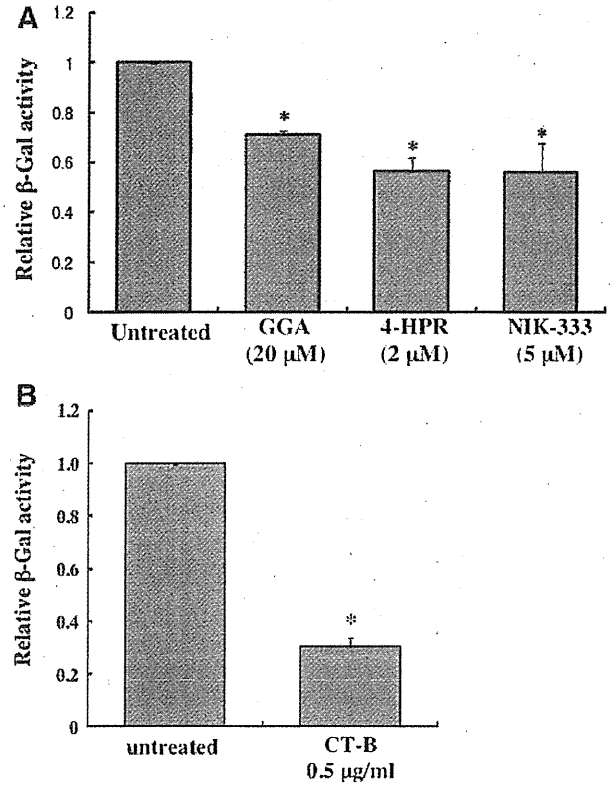

FIG. 6. Retinoid analogs and CT-B inhibit CXCR4-tropic HIV-1 Env-induced syncytium formation. Cell fusion activity of the HXB2 HIV-1 Env protein was measured in untreated and retinoid analog- **(A)** or CT-B-treated **(B)** cells (see Materials and Methods). The β-Gal activities in untreated cells were set to 1. These experiments were repeated in triplicate, and results are shown as the mean+SD. Asterisks indicate statistically significant differences compared to untreated cells.

too low to inhibit HIV-1 infection.[31] Similar to our results with CT-B, pertussis toxin B subunit also inhibits HIV-1 infection.[45–47] Although the receptor for pertussis toxin B oligomer has not yet been identified, the receptor appears to belong to a class of sialylated glycoproteins, with likely candidates being a 43-kDa protein[48] and CD11b/CD18 integrin.[49] Because the CT-B receptor GM1 is not the pertussis toxin B subunit receptor, the mechanisms by which these bacterial toxin B subunits inhibit HIV-1 infection appear to be different.

One route of HIV-1 transmission is through anal sex. As such, if gut bacteria that secrete nontoxic CT-B are present in the rectum, HIV-1 transmission through this route may be suppressed. Gut bacteria genetically engineered to express CT-B may be a useful novel low-cost strategy to prevent HIV-1 transmission through anal sex.

Use of these factors *in vivo*, however, should be approached cautiously. First, our study suggests that the acyclic retinoid analogs modulate cell surface expression of CD4 and CXCR4. Second, CT-B is used as an adjuvant for vaccination.[50,51] Therefore, these agents may induce unexpected effects *in vivo* via activation or perturbation of the human immune system. Further study is required to address this issue.

Other retinoid analogs have been reported to reduce cell surface expression of CXCR4,[52,53] similar to the retinoid analogs

used in this study. This down-regulation of CXCR4 expression is one of the mechanisms by which retinoid analogs inhibit CXCR4-tropic HIV-1 infection. HIV-1 infection is suppressed and influenza virus infection is elevated by 4-HPR through activation of endocytosis[23] without suppression of CXCR4 expression. In this study, VSV-G-mediated infection, which occurs via the endosomes, was not affected by the retinoid analogs. Further study is needed to understand the mechanism of HIV-1 infection inhibition by the retinoid analogs.

The retinoid analogs inhibited CXCR4 expression, while CT-B did not, suggesting that the mechanism of HIV-1 infection inhibition by CT-B differs from that by the retinoid analogs. Interestingly, CT-B inhibited CXCR4-tropic HIV-1 infection but not CCR5-tropic infection. Thus, CT-B may inhibit CXCR4-tropic HIV-1 entry at some point between virion binding to host cells and membrane fusion. CD4 and CCR5, but not CXCR4,[4–6] localize to lipid raft microdomains and constitutively interact.[54,55] It has been reported that CCR5-tropic HIV-1 infection is not dependent upon raft localization of CD4 and CCR5.[56] These results, together with our findings, suggest that CT-B inhibits the HIV-1 Env-induced interaction of CD4 and CXCR4 in lipid rafts and that raft microdomains are differentially involved in CXCR4- and CCR5-tropic HIV-1 infections. CT-B may have no effect on CCR5-tropic HIV-1 infection, because CD4 and CCR5 constitutively interact without binding HIV-1 Env. Recruitment of CXCR4 to CD4-containing raft microdomains by HIV-1 Env, however, has been observed in studies using CT-B as the raft marker.[5,6] Further study is required to understand the mechanism by which CT-B inhibits HIV-1 infection.

The plant sterol stigmasterol did not suppress HIV-1 vector infection. Our group previously reported that MβCD inhibits HIV-1 vector infection and that the addition of cholesterol to the MβCD-treated cells at 50 μg/ml for 30 min recovers infection, suggesting that cholesterol is incorporated into the cell membrane by the addition of cholesterol.[4] Therefore, treatment of cells with stigmasterol at 80 μg/ml for 24 h likely induces uptake of the plant sterol to the cell membrane. These results indicate that this plant sterol does not affect HIV-1 infection. Similar to mammalian cells, plant cells also have lipid raft microdomains in their membranes,[57] and these raft domains are enriched with plant sterols. Therefore, even upon replacement of cholesterol with stigmasterol in mammalian cells, the lipid raft structure is maintained, and HIV-1 infection remains unaffected.

In summary, the acyclic retinoid analogs, GGA and NIK-333, as well as CT-B, efficiently suppress HIV-1 vector infection. Another retinoid analog, 4-HPR, inhibits HIV-1 infection[23] but induces a vitamin A-deficiency syndrome. In contrast, NIK-333 induces no clinical side effects in patients with liver cancer.[28,29] This study suggests that NIK-333 can be used as a novel anti-HIV-1 agent without severe side effects. Additionally, CT-B inhibits CXCR4-tropic, but not CCR5-tropic.

HIV-1 infection, suggesting that host cell lipid raft microdomains are differentially involved in CXCR4- and CCR5-tropic HIV-1 infections.

Acknowledgments

We thank Dr. Y. Yokomaku for the HXB2 and JRFL Env expression plasmids and Dr. H. Hoshino for the NP2/CD4/X4 and NP2/CD4/R5 cells. We also thank Ms. Y. Kobayashi and Ms. F. Tsujita for assistance with laboratory work. This study was supported by the Japan Society for the Promotion of Science (JSPS) (No. 09J07637), a Health Science Research Grant from the Ministry of Health, Labor, and Welfare of Japan, and Kowa Company, Ltd. H. Kamiyama is a special research fellow of JSPS.

Author Disclosure Statement

No competing financial interests exist.

References

1. Kolber MA: Development of drug resistance mutations in patients on highly active antiretroviral therapy: Does competitive advantage drive evolution. AIDS Rev 2007;9: 68–74.
2. Carter GC, Bernstone L, Sangani D, Bee JW, Harder T, and James W: HIV entry in macrophages is dependent on intact lipid rafts. Virology 2009;386:192–202.
3. Del Real G, Jimenez-Baranda S, Lacalle RA, *et al.*: Blocking of HIV-1 infection by targeting CD4 to nonraft membrane domains. J Exp Med 2002;196:293–301.
4. Kamiyama H, Yoshii H, Tanaka Y, Sato H, Yamamoto N, and Kubo Y: Raft localization of CXCR4 is primarily required for X4-tropic human immunodeficiency virus type 1 infection. Virology 2009;386:23–31.
5. Manes S, del Real G, Lacalle RA, *et al.*: Membrane raft microdomains mediate lateral assemblies required for HIV-1 infection. EMBO Rep 2000;1:190–196.
6. Popik W, Alce TM, and Au WC: Human immunodeficiency virus type 1 uses lipid raft-colocalized CD4 and chemokine receptors for productive entry into CD4(+) T cells. J Virol 2002;76:4709–4722.
7. Michel V and Bakovic M: Lipid rafts in health and disease. Biol Cell 2007;99:129–140.
8. Waheed AA, Ablan SD, Mankowski MK, *et al.*: Inhibition of HIV-1 replication by amphotericin B methyl ester: Selection for resistant variants. J Biol Chem 2006;281:28699–28711.
9. Giguere JF and Tremblay MJ: Statin compounds reduce human immunodeficiency virus type 1 replication by preventing the interaction between virion-associated host intercellular adhesion molecule 1 and its natural cell surface ligand LFA-1. J Virol 2004;78:12062–12065.
10. del Real G, Jimenez-Baranda S, Mira E, *et al.*: Statins inhibit HIV-1 infection by down-regulating Rho activity. J Exp Med 2004;200:541–547.
11. Puri A, Rawat SS, Lin HM, *et al.*: An inhibitor of glycosphingolipid metabolism blocks HIV-1 infection of primary T-cells. AIDS 2004;18:849–858.
12. Mizrachi Y, Lev M, Harish Z, Sundaram SK, and Rubinstein A: L-Cycloserine, an inhibitor of sphingolipid biosynthesis, inhibits HIV-1 cytopathic effects, replication, and infectivity. J Acquir Immune Defic Syndr Hum Retrovirol 1996;11: 137–141.
13. Hug P, Lin HM, Korte T, *et al.*: Glycosphingolipids promote entry of a broad range of human immunodeficiency virus type 1 isolates into cell lines expressing CD4, CXCR4, and/or CCR5. J Virol 2000;74:6377–6385.
14. Erdreich-Epstein A, Tran LB, Bowman NN, *et al.*: Ceramide signaling in fenretinide-induced endothelial cell apoptosis. J Biol Chem 2002;277:49531–49537.
15. Maurer BJ, Metelitsa LS, Seeger RC, Cabot MC, and Reynolds CP: Increase of ceramide and induction of mixed apoptosis/necrosis by N-(4-hydroxyphenyl)-retinamide

in neuroblastoma cell lines. J Natl Cancer Inst 1999;91: 1138–1146.
16. O'Donnell PH, Guo WX, Reynolds CP, and Maurer BJ: N-(4-Hydroxyphenyl)retinamide increases ceramide and is cytotoxic to acute lymphoblastic leukemia cell lines, but not to non-malignant lymphocytes. Leukemia 2002;16:902–910.
17. Wang H, Maurer BJ, Reynolds CP, and Cabot MC: N-(4-Hydroxyphenyl)retinamide elevates ceramide in neuroblastoma cell lines by coordinate activation of serine palmitoyltransferase and ceramide synthase. Cancer Res 2001;61: 5102–5105.
18. Wiegandt H, Helland R, and Radsak K: Retinoic acid alters the metabolic 3H-labelling of glycosphingolipids. Biochem Biophys Res Commun 1987;143:525–531.
19. Finnegan CM, Rawat SS, Puri A, Wang JM, Ruscetti FW, and Blumenthal R: Ceramide, a target for antiretroviral therapy. Proc Natl Acad Sci USA 2004;101:15452–15457.
20. Clarke CJ, Mediwala K, Jenkins RW, Sutton CA, Tholanikunnel BG, and Hannun YA: Neutral sphingomyelinase-2 mediates growth arrest by retinoic acid through modulation of ribosomal S6 kinase. J Biol Chem 2011;286:21565–21576.
21. Nakashima H, Harada S, and Yamamoto N: Effect of retinoic acid on the replication of human immunodeficiency virus in HTLV-I-positive MT-4 cells. Med Microbiol Immunol 1987;176:189–198.
22. Anding AL, Chapman JS, Barnett DW, Curley RW Jr, and Clagett-Dame M: The unhydrolyzable fenretinide analogue 4-hydroxybenzylretinone induces the proapoptotic genes GADD153 (CHOP) and Bcl-2-binding component 3 (PUMA) and apoptosis that is caspase- dependent and independent of the retinoic acid receptor. Cancer Res 2007;67:6270–6277.
23. Finnegan CM and Blumenthal R: Fenretinide inhibits HIV infection by promoting viral endocytosis. Antiviral Res 2006; 69:116–123.
24. Sani BP and Meeks RG: Subacute toxicity of all-trans- and 13-cis-isomers of N-ethyl retinamide, N-2-hydroxyethyl retinamide, and N-4-hydroxyphenyl retinamide. Toxicol Appl Pharmacol 1983;70:228–235.
25. Shidoji Y and Ogawa H: Natural occurrence of cancer-preventive geranylgeranoic acid in medicinal herbs. J Lipid Res 2004;45:1092–1103.
26. Araki H, Shidoji Y, Yamada Y, Moriwaki H, and Muto Y: Retinoid agonist activities of synthetic geranyl geranoic acid derivatives. Biochem Biophys Res Commun 1995;209:66–72.
27. Okamoto K, Sakimoto Y, Imai K, Senoo H, and Shidoji Y: Induction of an incomplete autophagic response by cancer-preventive geranylgeranoic acid (GGA) in a human hepatoma-derived cell line. Biochem J 2011;440:63–71.
28. Muto Y, Moriwaki H, Ninomiya M, *et al.*: Prevention of second primary tumors by an acyclic retinoid, polyprenoic acid, in patients with hepatocellular carcinoma. Hepatoma Prevention Study Group. N Engl J Med 1996; 334:1561–1567.
29. Okusaka T, Ueno H, Ikeda M, and Morizane C: Phase I and pharmacokinetic clinical trial of oral administration of the acyclic retinoid NIK-333. Hepatol Res 2011;41:542–552.
30. Baumgartner S, Mensink RP, and Plat J: Plant sterols and stanols in the treatment of dyslipidemia: New insights into targets and mechanisms related to cardiovascular risk. Curr Pharm Des 2011;17:922–932.
31. Gauthier S and Tremblay MJ: Cholera toxin inhibits HIV-1 replication in human colorectal epithelial HT-29 cells through adenylate cyclase activation. Antiviral Res 2011;88: 207–216.
32. Hammache D, Pieroni G, Yahi N, *et al.*: Specific interaction of HIV-1 and HIV-2 surface envelope glycoproteins with monolayers of galactosylceramide and ganglioside GM3. J Biol Chem 1998;273:7967–7971.
33. Soda Y, Shimizu N, Jinno A, *et al.*: Establishment of a new system for determination of coreceptor usages of HIV based on the human glioma NP-2 cell line. Biochem Biophys Res Commun 1999;258:313–321.
34. Kubo Y, Yokoyama M, Yoshii H, *et al.*: Inhibitory role of CXCR4 glycan in CD4-independent X4-tropic human immunodeficiency virus type 1 infection and its abrogation in CD4-dependent infection. J Gen Virol 2007;88:3139–3144.
35. Kubo Y, Yoshii H, Kamiyama H, *et al.*: Ezrin, Radixin, and Moesin (ERM) proteins function as pleiotropic regulators of human immunodeficiency virus type 1 infection. Virology 2008;375:130–140.
36. Tobiume M, Takahoko M, Tatsumi M, and Matsuda M: Establishment of a MAGI-derived indicator cell line that detects the Nef enhancement of HIV-1 infectivity with high sensitivity. J Virol Methods 2001;97:151–158.
37. Tanaka R, Yoshida A, Murakami T, *et al.*: Unique monoclonal antibody recognizing the third extracellular loop of CXCR4 induces lymphocyte agglutination and enhances human immunodeficiency virus type 1-mediated syncytium formation and productive infection. J Virol 2001;75:11534–11543.
38. Maciaszek JW, Coniglio SJ, Talmage DA, and Viglianti GA: Retinoid-induced repression of human immunodeficiency virus type 1 core promoter activity inhibits virus replication. J Virol 1998;72:5862–5869.
39. Hanley TM, Kiefer HL, Schnitzler AC, Marcello JE, and Viglianti GA: Retinoid-dependent restriction of human immunodeficiency virus type 1 replication in monocytes/macrophages. J Virol 2004;78:2819–2830.
40. Kiefer HL, Hanley TM, Marcello JE, Karthik AG, and Viglianti GA: Retinoic acid inhibition of chromatin remodeling at the human immunodeficiency virus type 1 promoter. Uncoupling of histone acetylation and chromatin remodeling. J Biol Chem 2004;279:43604–43613.
41. Chatterjee A, Bosch RJ, Hunter DJ, Manji K, Msamanga GI, and Fawzi WW: Vitamin A and vitamin B-12 concentrations in relation to mortality and morbidity among children born to HIV-infected women. J Trop Pediatr 2011;56:27–35.
42. Humphrey JH, Iliff PJ, Marinda ET, *et al.*: Effects of a single large dose of vitamin A, given during the postpartum period to HIV-positive women and their infants, on child HIV infection, HIV-free survival, and mortality. J Infect Dis 2006; 193:860–871.
43. Mehta S and Fawzi W: Effects of vitamins, including vitamin A, on HIV/AIDS patients. Vitam Horm 2007;75:355–383.
44. Semba RD, Ndugwa C, Perry RT, *et al.*: Effect of periodic vitamin A supplementation on mortality and morbidity of human immunodeficiency virus-infected children in Uganda: A controlled clinical trial. Nutrition 2005;21: 25–31.
45. Iordanskiy S, Iordanskaya T, Quivy V, Van Lint C, and Bukrinsky M: B-oligomer of pertussis toxin inhibits HIV-1 LTR-driven transcription through suppression of NF-kappaB p65 subunit activity. Virology 2002;302:195–206.
46. Alfano M, Schmidtmayerova H, Amella CA, Pushkarsky T, and Bukrinsky M: The B-oligomer of pertussis toxin deacti-

vates CC chemokine receptor 5 and blocks entry of M-tropic HIV-1 strains. J Exp Med 1999;190:597–605.
47. Alfano M, Pushkarsky T, Poli G, and Bukrinsky M: The B-oligomer of pertussis toxin inhibits human immunodeficiency virus type 1 replication at multiple stages. J Virol 2000;74:8767–8770.
48. Rogers TS, Corey SJ, and Rosoff PM: Identification of a 43-kilodalton human T lymphocyte membrane protein as a receptor for pertussis toxin. J Immunol 1990;145:678–683.
49. Wong WS, Simon DI, Rosoff PM, Rao NK, and Chapman HA: Mechanisms of pertussis toxin-induced myelomonocytic cell adhesion: Role of Mac-1(CD11b/CD18) and urokinase receptor (CD87). Immunology 1996;88:90–97.
50. Kang SM, Yao Q, Guo L, and Compans RW: Mucosal immunization with virus-like particles of simian immunodeficiency virus conjugated with cholera toxin subunit B. J Virol 2003;77:9823–9830.
51. Sun JB, Czerkinsky C, and Holmgren J: Mucosally induced immunological tolerance, regulatory T cells and the adjuvant effect by cholera toxin B subunit. Scand J Immunol 2011; 71:1–11.
52. Villablanca EJ, Zhou D, Valentinis B, *et al.:* Selected natural and synthetic retinoids impair CCR7- and CXCR4-dependent cell migration in vitro and in vivo. J Leukoc Biol 2008; 84:871–879.
53. Matsumoto T, Jimi S, Hara S, Takamatsu Y, Suzumiya J, and Tamura K: Am80 inhibits stromal cell-derived factor-1-induced chemotaxis in T-cell acute lymphoblastic leukemia cells. Leuk Lymphoma 2011;51:507–514.
54. Baker AM, Sauliere A, Gaibelet G, *et al.:* CD4 interacts constitutively with multiple CCR5 at the plasma membrane of living cells. A fluorescence recovery after photobleaching at variable radii approach. J Biol Chem 2007;282:35163–35168.
55. Gaibelet G, Planchenault T, Mazeres S, *et al.:* CD4 and CCR5 constitutively interact at the plasma membrane of living cells: A confocal fluorescence resonance energy transfer-based approach. J Biol Chem 2006;281:37921–37929.
56. Percherancier Y, Lagane B, Planchenault T, *et al.:* HIV-1 entry into T-cells is not dependent on CD4 and CCR5 localization to sphingolipid-enriched, detergent-resistant, raft membrane domains. J Biol Chem 2003;278:3153–3161.
57. Lefebvre B, Furt F, Hartmann MA, *et al.:* Characterization of lipid rafts from Medicago truncatula root plasma membranes: a proteomic study reveals the presence of a raft-associated redox system. Plant Physiol 2007;144:402–418.

Address correspondence to:
Yoshinao Kubo
Division of Cytokine Signaling
Graduate School of Biomedical Sciences
Nagasaki University
1-12-4 Sakamoto
Nagasaki 852-8523
Japan

E-mail: yoshinao@nagasaki-u.ac.jp

DNA AND CELL BIOLOGY
Volume 31, Number 11, 2012

Pp. 1636–1644
DOI: 10.1089/dna.2012.1666

Serum Starvation Activates NF-κB Through G Protein β2 Subunit-Mediated Signal

Tomoko Kohno, Yoshinao Kubo, Kiyoshi Yasui, Megumi Haraguchi, Sayuri Shigematsu, Koon Jiew Chua, Toshifumi Matsuyama, and Hideki Hayashi

Several cell stresses induce nuclear factor-kappaB (NF-κB) activation, which include irradiation, oxidation, and UV. Interestingly, serum-starving stress-induced NF-κB activation in COS cells, but not in COS-A717 cells. COS-A717 is a mutant cell line of COS cells that is defective of the NF-κB signaling pathway. We isolated genes with compensating activity for the NF-κB pathway and one gene encoded the G protein β2 (Gβ2). Gβ2 is one of the G protein-coupled receptor signaling effectors. In COS-A717 cells, Gβ2 expression is significantly reduced. In Gβ2 cDNA-transfected COS-A717 cells, the NF-κB activity was increased along with the recovery of Gβ2 expression. Furthermore, serum-starving stress induced the NF-κB activity in Gβ2-transfected COS-A717 cells. Consistently, the serum-starved COS cells with siRNA-reduced Gβ2 protein expression showed decreased NF-κB activity. These results indicate that Gβ2 is required for starvation-induced NF-κB activation and constitutive NF-κB activity. We propose that serum contains some molecule(s) that strongly inhibits NF-κB activation mediated through Gβ2 signaling.

Introduction

Nuclear factor-kappaB (NF-κB) is a ubiquitously expressed transcription factor with critical roles in cell survival, proliferation, apoptosis, immune response, and inflammation. NF-κB usually exists as a heterodimer of p50 and p65 (Rel A), and is kept in the cytoplasm through an association with inhibitor of kappaB (IκB) inhibitory proteins. After various stimulations, the serine residues at positions 32 (S32) and 36 (S36) in the IκB proteinare phosphorylated (Brown *et al.*, 1995) by the IκB kinase (IKK) complex (Zandi *et al.*, 1997), and the IκB protein is degraded by the ubiquitin–proteasome pathway (Chen *et al.*, 1995). The IKK complex consists of two catalytic subunits, IKK1 and IKK2 (also referred to as IKKα and IKKβ), and a regulatory subunit, NEMO (Yamaoka *et al.*, 1998). Cytokines and various cell stresses, including irradiation (Criswell *et al.*, 2003), oxidation (Marshall *et al.*, 2000), and UV (Kato *et al.*, 2003), induce NF-κB activation. Serum starvation also activates NF-κB in various cell lines (Ryter and Gomer, 1993; Grimm *et al.*, 1996), indicating that serum contains unknown inhibitor(s) of NF-κB.

On the other hand, constitutively active NF-κB exists in certain normal cells (Pagliari *et al.*, 2000; Lilienbaum and Israel, 2003) and several tumor cells without stimulation (Mori *et al.*, 1999; Lind *et al.*, 2001). However, the mechanism by which NF-κB is constitutively activated in these cells is not known. COS cells have a relatively high level of basal NF-κB activity. We established a mutant cell line, COS-A717, with a defective NF-κB signaling pathway (Kohno *et al.*, 2008). The basal level of NF-κB activity in the COS-A717 cells was reduced by as much as sevenfold, as compared with that in the parental COS cells. Serum starvation induced NF-κB activation in the parental COS cell line, but not in the COS-A717 cell clone. Since the COS-A717 cell clone was constructed by the treatment of COS cells with a frameshift-inducing agent, it is most likely that the NF-κB activating factor(s) expressed in the parental COS cells is not functional in the COS-A717 cells. We previously isolated the B cell activating factor of the TNF family (BAFF) receptor as an NF-κB activator in COS-A717 cells (Kohno *et al.*, 2008). However, the original COS cells do not express BAFF-R, indicating that BAFF-R is not responsible for the defective NF-κB signaling in the COS-A717 cells, and activates NF-κB through a salvage pathway.

In this study, we isolated the guanine nucleotide-binding protein β2 subunit (Gβ2) cDNA as another NF-κB activator by screening a human spleen cDNA expression library. The guanine nucleotide-binding proteins (G proteins) are signal transducers required for various G protein coupled receptor (GPCR)-effector networks (Xie *et al.*, 2000; Wu *et al.*, 2001; Albert and Robillard, 2002). GPCRs 'transduce signals through heteromeric G proteins, and several of them activate NF-κB (Xie *et al.*, 2000; Grabiner *et al.*, 2007; Sun *et al.*, 2009). The heteromeric G proteins consist of α, β, and γ subunits,

Division of Cytokine Signaling, Department of Molecular Microbiology and Immunology, Graduate School of Biomedical Sciences, Nagasaki University, Nagasaki, Japan.

and the α subunit has GTPase activity. When GPCRs interact with their ligands, the active GTP-bound α subunit is released from the heteromeric G protein complex, and Gα and Gβγ induce downstream signaling (Stephens *et al.*, 1994). The Gβ2 expression level in the parental COS cells is much higher than that in the mutant COS-A717 cells. Transfection of a Gβ2 expression plasmid activated NF-κB in COS-A717 cells. The knockdown of Gβ2 expression by siRNA in COS and HT1080 cells reduced the basal NF-κB activity. These results indicate that the activation of the GPCR signal pathway by Gβ2 results in constitutive NF-κB activation in the transformed cells, and the defect of Gβ2 expression is one of the determinants for reduced NF-κB activity in the COS-A717 mutant cells.

Serum starvation activates NF-κB in COS cells, but not in COS-A717 cells. Transfection of COS-A717 cells with Gβ2 restored the starvation-induced NF-κB activation. These results show that NF-κB activation by serum starvation occurs through the Gβ2 signaling pathway, and the inhibitor(s) present in serum sppress the Gβ2 signal. Taken together, our findings suggest that the constitutive NF-κB activation in transformed cells is induced by the GPCR signaling pathway through Gβ2, and that serum contains factor(s) reducing NF-κB activity by suppressing the GPCR signaling.

Materials and Methods

Plasmids and reagents

The human spleen cDNA library was purchased from Life Technologies. The five-tandem κB luciferase reporter vector (5×κB luciferase) was purchased from Stratagene. The IκBα superrepressor (IκBα-SR) expression plasmid was described previously (Sugita *et al.*, 2002). The expression vectors for the dominant negative forms of IKK1 (IKK1.DN), IKK2 (IKK2.DN), and NEMO (NEMO.DN) were kind gifts from Dr. Yamaoka (Tokyo Medical and Dental University, Tokyo, Japan) (Hironaka *et al.*, 2004). The expression vector for the dominant negative mutant of Akt (Akt.DN) was generously provided by Dr. V. Stambolic (Ontario Cancer Institute, Toronto, Canada). Wortmannin was purchased from Sigma.

Cells

The mutant cell lines COS-A717 and COS-A717-GS were described previously (Kohno *et al.*, 2008). The mouse spleen cells were obtained from a C57BL/6 mouse. COS (Kohno *et al.*, 2008), HT1080 (Jones *et al.*, 1975), and HEK293T cells were maintained in the Dulbecco's modified Eagle's medium, and ST1 cells (Yamada, 1996) were maintained in the RPMI1640 medium containing 10% heat-inactivated fetal bovine serum (FBS) at 37°C in a humidified 5% CO_2 atmosphere.

Expression cloning of Gβ2

Isolation of genes with compensating activity for the NF-κB activation pathway was performed according to the previously described method (Kohno *et al.*, 2008). Briefly, COS-A717-GS cells were transfected with a human spleen cDNA library (Life Technologies) using the FuGene 6 reagent. After 48 h of transfection, the top 0.5% fraction of fluorescent cells was collected using a FACStar Plus (Becton, Dickinson and Co.). Plasmids were extracted from sorted cells (Hirt, 1967), amplified in bacteria, and used in three subsequent rounds of flow cytometry-based enrichment. Individual bacterial colonies obtained from the third sorting were grouped into pools of 50 colonies. Positive pools were subdivided further into subpools with half the number of colonies, and were subjected to repeated screening. This process finally yielded independent clones that conferred compensation for the NF-κB activation pathway in COS-A717 cells.

Transfection and luciferase assay

Cells were transfected with a 5×κB-luciferase reporter and a Gβ2 expression plasmid, as indicated in the text and figure legends. Transient transfections were performed using the FuGene 6 reagent (Roche). When necessary, additional DNA (pcDNA3.1) was added to equalize the amount of transfected DNA in each sample. At 48 h post-transfection, the κB-directed expression of firefly luciferase was determined, using luciferase assay reagents (Promega), and the luciferase activities were measured with a BioOrbit 1254 luminometer. The relative transfection efficiency in each sample was determined by measuring the Renilla luciferase activity. The data were normalized per transfection efficiency. Data shown are averages and SD from three independent experiments.

Western blot analysis

Cell extracts were prepared from the cells transfected for the luciferase assay. Cell lysates were resolved by 12.5% SDS PAGE, transferred onto an Immobilon-P membrane (Millipore), and blocked with 5% nonfat dry milk in TBS with 0.5% Tween 20. The blots were incubated with anti-Gβ2, anti-IKK1, anti-IKK2, anti-NEMO, anti-Akt1, anti- IκBα, and anti-phosho S32, and S36-containing peptide of IκBα antibodies (Santa Cruz Biotechnology; refer to Tables 1 and 2), or an anti-β-actin antibody (Chemicon), followed by an incubation with a horseradish peroxidase-conjugated goat anti-mouse or anti-rabbit Ig (Amersham Pharmacia Biotech). The blots were visualized with the ECL detection system (Amersham Pharmacia Biotech).

Electrophoretic mobility shift assay

Preparation of nuclear extracts for electrophoretic mobility shift assays (EMSAs) was performed as described previously (Sugita *et al.*, 2002). The consensus κB site 5′-AGTTGAGG GGACTTTCCCAGGC-3′ and mutant 5′-AGTTGAGGCGAC TTTCCCAGGC-3′ oligonucleotides were obtained from Santa Cruz Biotechnology. The double stranded oligonucleotides were end-labeled with [γ-^{32}P] ATP, using T4 polynucleotide kinase (Takara). The reaction was conducted in a total volume of 10 μL, using 10 μg of nuclear extract, 1 μg of poly(dI-dC), 20 mM HEPES-NaOH (pH 7.6), 100 mM NaCl, 1 mM DTT, 1 mM PMSF, and 2% glycerol. The binding reaction mixture was incubated with 10,000 cpm of radiolabeled probe for 15 min. For the competition and supershift assays, a 20-fold excess of unlabeled or mutant oligonucleotide, and the antibodies to p65 or p50 (Santa Cruz Biotechnology) were added to the reaction, respectively. The samples were loaded onto a 5% nondenaturing polyacrylamide gel, which was run in a 0.5×TBE buffer. After

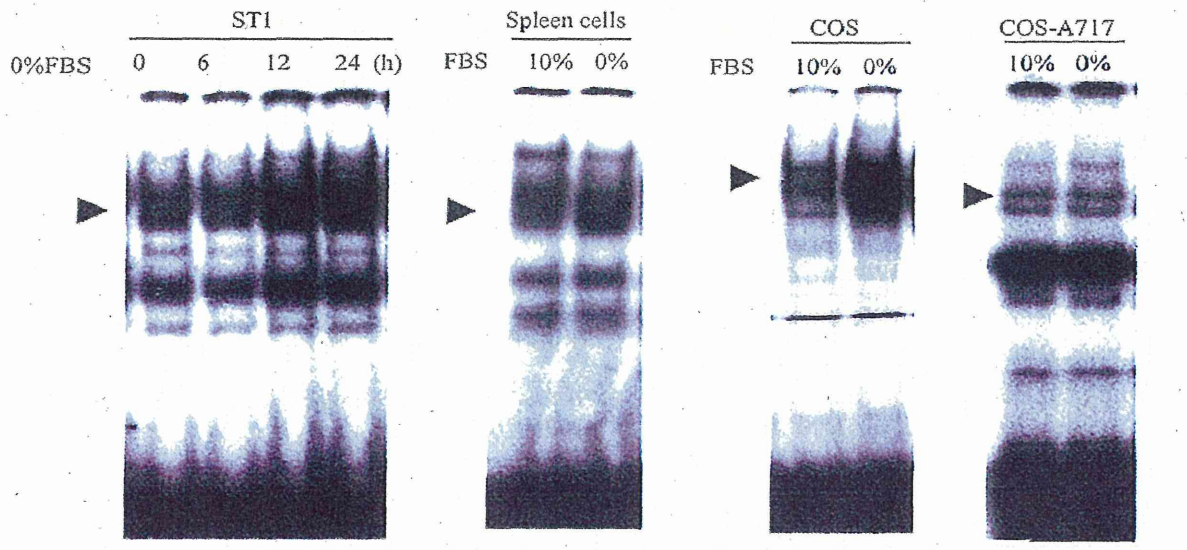

FIG. 1. Serum-starving stress-induced nuclear factor-kappaB (NF-κB) activation. The nuclear extracts were incubated with a ^{32}P-labeled NF-κB consensus oligonucleotide, and analyzed by an electrophoretic mobility shift assay. Nuclear cell extracts from ST1 cells, which were cultured without fetal bovine serum (FBS) for 0, 6, 12, 24 h (*ST1 panel*). The mouse spleen cells were cultured with 10% FBS or 0% FBS for 24 h (*Spleen cells panel*). Nuclear cell extracts from COS (*COS panel*) and COS-A717 (*COS-A717 panel*) cells, which were cultured with 10% FBS or 0% FBS for 24 h. The *arrowhead* indicates the NF-κB-containing complex.

electrophoresis, the gel was dried and processed for autoradiography.

siRNA

The nucleotide sequences of the two siRNAs for Gβ2 are as follows:

#1 sense 5′-CAUCUGCUCCAUCUACAGCdTdT-3′,
anti-sense 5′-GCUGUAGAUGGAGCAGAUGdTdT-3′;
#2 sense 5′-AGACCUUCAUCGGCCAUGAdTdT-3′,
anti-sense5′-UCAUGGCCGAUGAAGGUCUdGdT;

and sense 5′-GGCUACGUCCAGGAGCGCAdTdT-3′, antisense 5′-UGCGCUCCUGGACGUAGCCdTdT-3′ for GFP. The annealed oligonucleotides were transfected by using Lipofectamine 2000 (Invitrogen). Cells were maintained in the Dulbecco's modified Eagle's medium without FBS at the transfection. Cells were harvested after 24 and 48 h after the transfection for COS and HT1080 cells, respectively. For the luciferase assay, cells were transfected with the 5×κB-luciferase reporter using the FuGene 6 reagent, at 6 h after the siRNA transfection.

Results

Serum-starving stress induces NF-κB activation

Cell stresses, such as irradiation, UV, and oxidation (Supplementary Fig. S1; Supplementary Data are available online at www.liebertpub.com/dna), induce NF-κB activation. Cells are usually cultured with 10% FBS in medium *in vitro*. Serum includes various factors and nutrients for cell survival and proliferation, and thus serum starvation ceases cell proliferation, and then induces cell death. Serum may include factors affecting NF-κB signaling. To address this issue, we analyzed the effects of serum starvation on NF-κB binding to the target sequence by EMSA of nuclear extracts from several cell lines (ST1, COS, and COS-A717) and mouse primary spleen cells. The binding of NF-κB to the target sequence was enhanced by serum starvation in all examined cells, except for the mutant COS-A717 cells, which exhibit defective NF-κB signaling (Fig. 1). These results indicate that serum starvation induces NF-κB activation, suggesting that serum contains unknown factor(s) inhibiting NF-κB activity.

Expression cloning of an NF-κB activating molecule using COS-A717 cells

Many transformed cell lines containing the COS cell line have constitutively activated NF-κB signaling. To identify NF-κB activators in the COS cells, a COS-A717 cell derivative containing the GFP gene under the control of the Sp1 site-deleted HIV-1 LTR was constructed, and the cells were designated as COS-A717-GS. The GFP is expressed by NF-κB activation in the COS-A717-GS cells, because the expression from the Sp1 site-deleted HIV-1 LTR is NF-κB dependent. The COS-A717-GS cells were transfected with a human spleen cDNA expression library, and GFP-expressing cells were selected (Fig. 2A). The sequence analysis of the cDNA expressed in the GFP-positive COS-A717-GS cells revealed that it perfectly matched the Gβ2. The expression level of the Gβ2 protein in COS-A717 cells was much lower than that in the parental COS cells (Fig. 2B).

To confirm that Gβ2 activates NF-κB activity, COS and COS-A717 cells were transfected with the Gβ2 expression plasmid, and the NF-κB promoter activity was measured using the 5×κB-luciferase plasmid. Gβ2 activated the NF-κB promoter activity in both COS and COS-A717 cells, in a dose-dependent manner (Fig. 2C). Transfection of the COS-A717 mutant cells with the Gβ2 expression plasmid (0.5 μg) resored the NF-κB activity comparable to the parental COS cells (sevenfold). When 0.5 μg of the Gβ2 expression plasmid was transfected

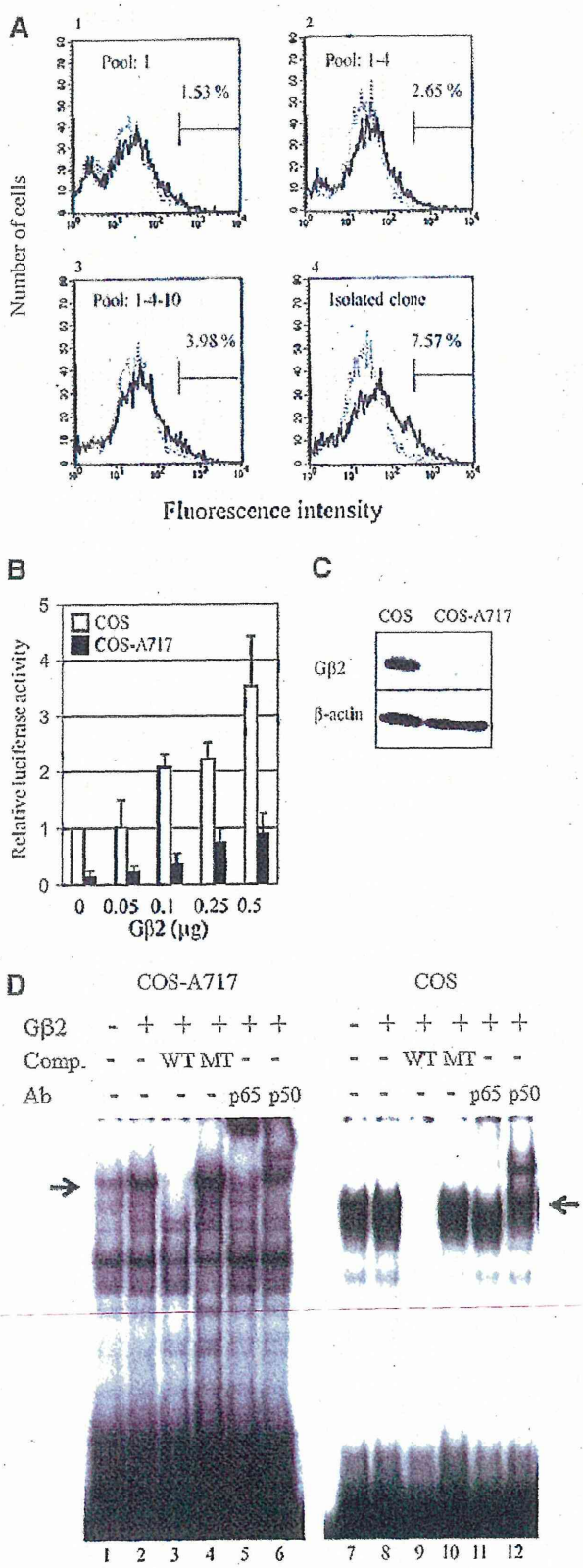

into the COS cells, the NF-κB activity was also increased by threefold. The DNA-binding activity of NF-κB was elevated by Gβ2 by about 1.7- and 6.2-fold in COS and COS-A717 cells, respectively (Fig. 3D). The complex formation was inhibited by a wild-type κB oligonucleotide competitor, but not by a mutant κB oligonucleotide. The complex was supershifted by both anti-p65 and -p50 antibodies, indicating that the complex consisted of p65 and p50 (Fig. 3D). The Gβ2 transfection activated the NF-κB signal more efficiently in the mutant COS-A717 cells than in the COS cells that originally express Gβ2. These results indicate that Gβ2 activates NF-κB signaling and the defect of Gβ2 expression is one of the determinants for the reduced NF-κB activity in the COS-A717 cells.

Gβ2 is required for NF-κB activation induced by serum starvation

Serum starvation activated NF-κB by 10-fold in COS cells, but had no effect in COS-A717 cells (Fig. 3A). Since the level of the Gβ2 protein is much lower in the COS-A717 cells than in the parental COS cells, we examined whether Gβ2 was involved in the NF-κB activation by serum starvation. Serum starvation elevated the NF-κB activity by fourfold in the Gβ2-transfected COS-A717 cells, indicating that Gβ2 is required for the serum starvation-induced NF-κB activation and that the Gβ2-activated signal is inhibited by the unknown factor(s) present in serum. However, because the level of NF-κB activity in the starved Gβ2-expressing COS-A717 cells was lower than that in the starved COS cells, the COS-A717 cells have additional defect(s) in the NF-κB signal activation.

FIG. 2. G protein β2 (Gβ2) activates NF-κB. **(A)** Identification of Gβ2 by expression cloning. **(A-1)** COS-A717-GS cells were transfected with plasmids obtained from a positive pool of 50 bacterial transformants (pool 1) following four rounds of FACS enrichment. **(A-2)** COS-A717-GS cells were transfected with plasmids from a positive pool (1-4), containing 20 bacteria colonies. **(A-3)** COS-A717-GS cells were transfected with plasmids from a positive pool (1-4-10), containing 10 bacterial colonies. **(A-4)** COS-A717 GS cells were transfected with a Gβ2-encoding clone. **(B)** Western blot analysis of Gβ2 in COS and COS-A717 cells. Proteins were analyzed by immunoblotting with an anti-Gβ2 Ab (*top*) and an anti-β-actin Ab (*bottom*). **(C)** Gβ2-mediated NF-κB activation in COS-A717 cells. COS and COS-A717 cells were transiently transfected with 0.25 μg of the 5×κB-luciferase reporter and the Gβ2 expression construct (0.05, 0.1, 0.25, and 0.5 μg), and then additional DNA (pcDNA3) was added to make the total amount of DNA 1 μg/well. At 48 h post-transfection, the cells were harvested and the luciferase activity was measured. The relative transfection efficiency in each sample was determined by the measurement of the Renilla luciferase activity. The relative luciferase activity in control COS cells (without Gβ2) was set to 1.0. Data shown are averages +SD from three independent experiments. **(D)** Gβ2 induced the NF-κB-binding ability in COS-A717 cells and COS cells. Nuclear proteins from untransfected (*lanes* 1, 7) or Gβ2 transfected (*lanes* 2–6, 8–12) COS-A717 cells or COS cells were isolated. The unlabeled consensus κB oligonucleotide (*lanes* 3, 9) or the mutant κB oligonucleotide (*lanes* 4, 10) was added as a competitor in a 20-fold molar excess to the binding reaction. Abs against p65 (*lanes* 5, 11) and p50 (*lanes* 6, 12) were added to the reaction for a supershift assay. The *arrow* indicates the NF-κB-containing complex.

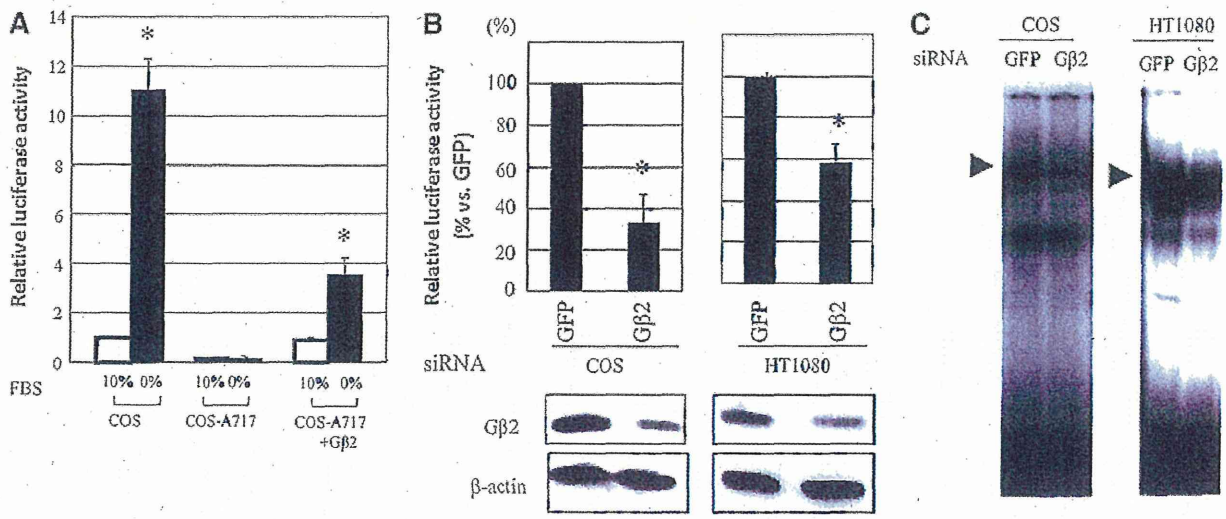

FIG. 3. Gβ2 is required for serum starvation-induced NF-κB activation and for constitutive NF-κB activation in transformed cells. **(A)** The serum-starving stress-induced NF-κB activation was analyzed by a luciferase assay. COS, COS-A717, and Gβ2-transfected COS-A717 cells were transiently transfected with the 5×κB-luciferase reporter. Six hours after transfection, the cells were washed with phosphate buffered saline (PBS) and incubated with (10%) or without FBS (0%) for 36 h for the luciferase assay. The luciferase activities in COS cells incubated with 10% FBS were set as 1.0. The activations were significant ($^*p < 0.05$). **(B)** The Gβ2 siRNA reduced the NF-κB activity in COS and HT1080 cells. The NF-κB activity was determined by transfection with the 5×κB-luciferase reporter together with the GFP or Gβ2 siRNA, and shown as the % of that in cells transfected with the GFP siRNA. Western blot analyses of Gβ2 (*top*) and β-actin (*bottom*) in cells transfected with the GFP or Gβ2 siRNA#1 were performed. The inhibitions were significant ($^*p < 0.05$). **(C)** Nuclear cell extracts were isolated from COS and HT1080 cells transfected with the GFP or Gβ2 siRNA. The *arrowhead* indicates the NF-κB-containing complex.

Gβ2 is involved in NF-κB in HT1080 human fibrosarcoma cell line

HT1080 cells also have a relatively high level of basal NF-κB activity. We examined whether Gβ2 contributes to the constitutive activation of NF-κB in HT1080 cells. Knockdown of Gβ2 expression by siRNA reduced the basal NF-κB activity not only in COS cells, but also in HT1080 cells (Fig. 3B). The siRNA against Gβ2 indeed reduced the Gβ2 protein level. Consistent with the κB promoter activity, the knockdown of Gβ2 inhibited the NF-κB-binding capability to the target sequence (Fig. 3C). These results indicate that Gβ2 is required for the constitutive activation of NF-κB in COS and HT1080 cells, suggesting that Gβ2-mediated signaling contributes to the constitutive NF-κB activation. The serum-deprived Gβ2-mediated NF-kB activation in COS cell was also confirmed using another siRNA (Supplementary Fig. S2).

Impact of IKKs, NEMO, and IκB in Gβ2-induced NF-κB activation

To determine whether the Gβ2 induced NF-κB activation requires IκB phosphorylation, a IκBα-SR with mutations at the inducible phosphorylation sites, S32G and S36A, was coexpressed with Gβ2 in COS-A717 cells. The IκB-SR abolished the Gβ2-induced NF-κB activation in a dose-dependent fashion (Fig. 4A). This result suggests that the phosphorylation of IκBα at S32 and S36 is necessary for the Gβ2-induced NF-κB activation. An important regulator of phosphorylation in the IκB pathway is the IKK complex, which comprises multiple kinases, including IKK1 (IKKα), IKK2 (IKKβ), and NEMO (IKKγ). We examined whether IKK1, IKK2, and/or NEMO were involved in the Gβ2-induced NF-κB activation. Dominant negative forms of IKK1 (IKK1.DN), IKK2 (IKK2.DN), and NEMO (NEMO.DN) were each coexpressed in the Gβ2-transfected COS-A717 cells. As shown in Figure 4B–D, IKK1.DN, IKK2.DN, and NEMO.DN were each able to reduce the Gβ2-induced NF-κB activation in COS-A717 cells in a dose-dependent fashion, indicating that IKK1, IKK2, and NEMO are involved in the Gβ2-induced NF-κB activation. Especially, the IKK2.DN more efficiently suppressed the Gβ2-mediated NF-κB activation than IKK1.DN and NEMO.DN. This result suggests that IKK2 plays an important role in the Gβ2-induced NF-κB activation, like the bradykinin-induced NF-κB activation through Gαq and Gβγ (Xie *et al.*, 2000). To confirm the expressions of the dominant negative and endogenous IKK1, IKK2, NEMO, IκBα, and Akt, COS cells were transfected with the mutant expressing plasmids, and the cell lysates were subjected to Western blotting analysis using their specific antibodies. The descriptions of the dominant negative mutants and their specific antibodies used here are summarized in the Tables 1 and 2, respectively. As shown in Figure 5A, we have confirmed that the anti-IKK1, NEMO, and Akt1 antibodies were able to detect the simian endogenous proteins as well as their human and mouse dominant negative mutants. On the other hand, the antibodies against IKK2 and IκBα reacted to their human dominant negative mutants and the human endogenous proteins in HEK293T cells, but not to the simian endogenous proteins. Considering the different affinities of the antibodies between endogenous simian proteins and their human or mouse counterparts, we could not assess precisely the relative amounts of dominant negative mutants to endogenous proteins in COS cells. However, each

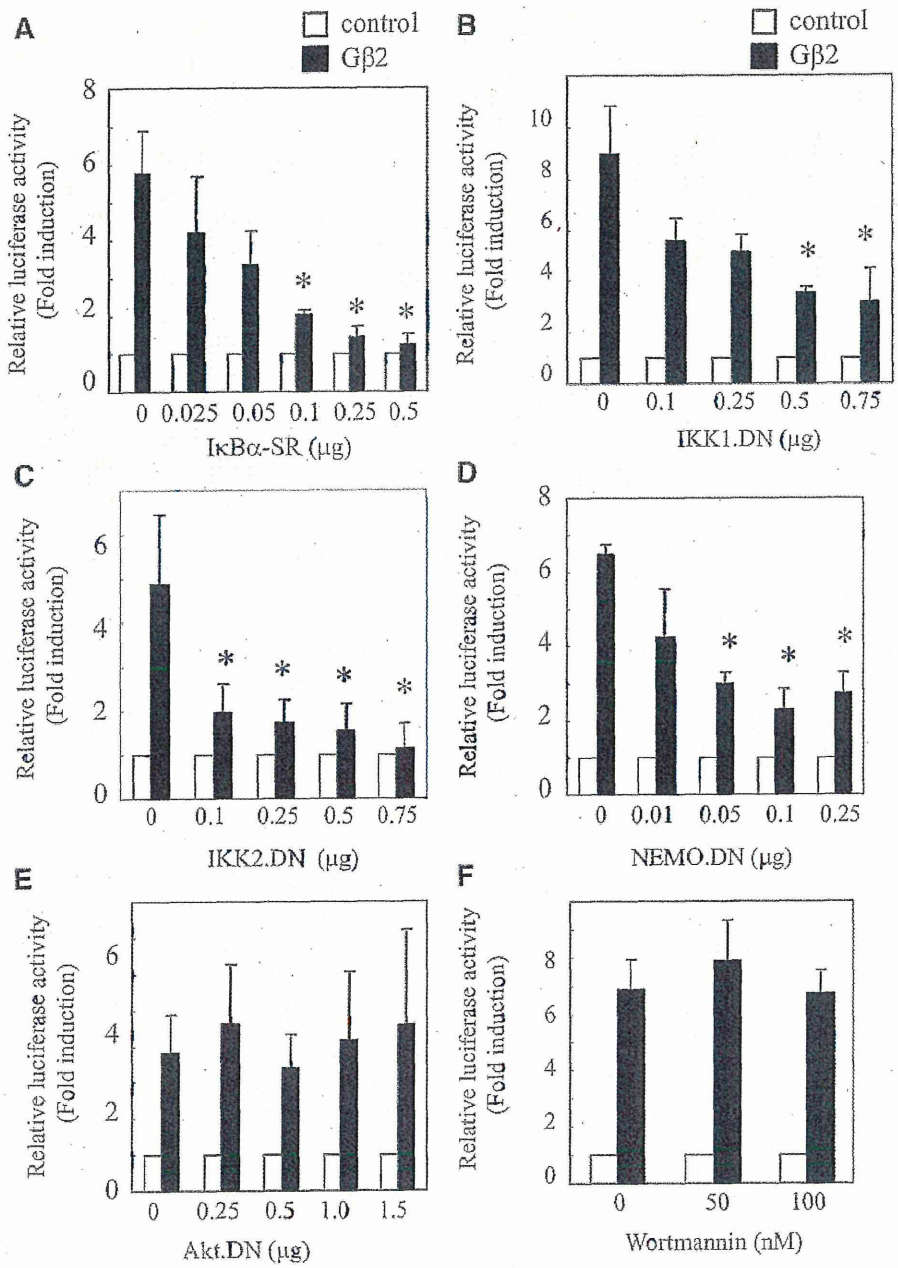

FIG. 4. Involvement of IκB, IκB kinase 1 (IKK1), IKK2, and NEMO in Gβ2-induced NF-κB activation. COS-A717 cells were transfected with 0.25 μg of the 5×κB-luciferase and the mutant expression plasmid of IκBα super-repressor (IκBα-SR) **(A)**, IKK1 (IKK1.DN) **(B)**, IKK2 (IKK2.DN) **(C)**, NEMO (NEMO.DN) **(D)**, or Akt (Akt.DN) **(E)**, together with the Gβ2 construct (0.25 μg) or pcDNA3.1. The pcDNA3.1 plasmid was added to make the total amount of DNA 1 μg/well. COS-A717 cells were cotransfected with 0.5 μg of the 5×κB-luciferase reporter without (control) or with 0.5 μg of the Gβ2 construct. Wortmannin was added 1 h before transfection **(F)**. The relative luciferase activity in the control cells without Gβ2 was set as 1.0. Data shown are averages and SD from three independent experiments. The inhibitions were significant ($^*p < 0.05$).

TABLE 1. CHARACTERISTICS OF THE DOMINANT NEGATIVE MUTANTS

Molecule	*Species*	*Structure*	*MW (kDa)*	*Tag*
IκBα	Human	S32G, S36A mutant	40	—
IKK1	Human	N145D mutant	85	VSV
IKK2	Human	N145D mutant	87	VSV
NEMO	Mouse	97–412 C-terminal fragment	37	VSV
Akt	Mouse	K179A, T308A, S473A mutant	69	–

MW, molecular weight.

TABLE 2. CHARACTERISTICS OF THE ANTIBODIES

Antigen	*Cross-reactivity*
Human IκBα C-terminal peptide	Human/mouse/rat
Human IKK1 full-length	Human/mouse/rat
Human IKK2 C-terminal peptide	Human/canine
Human NEMO full-length	Human/mouse/rat
Human Akt1 345–480 peptide	Human/mouse/rat
Human phospho-S32 and S36-containing peptide	Human/mouse

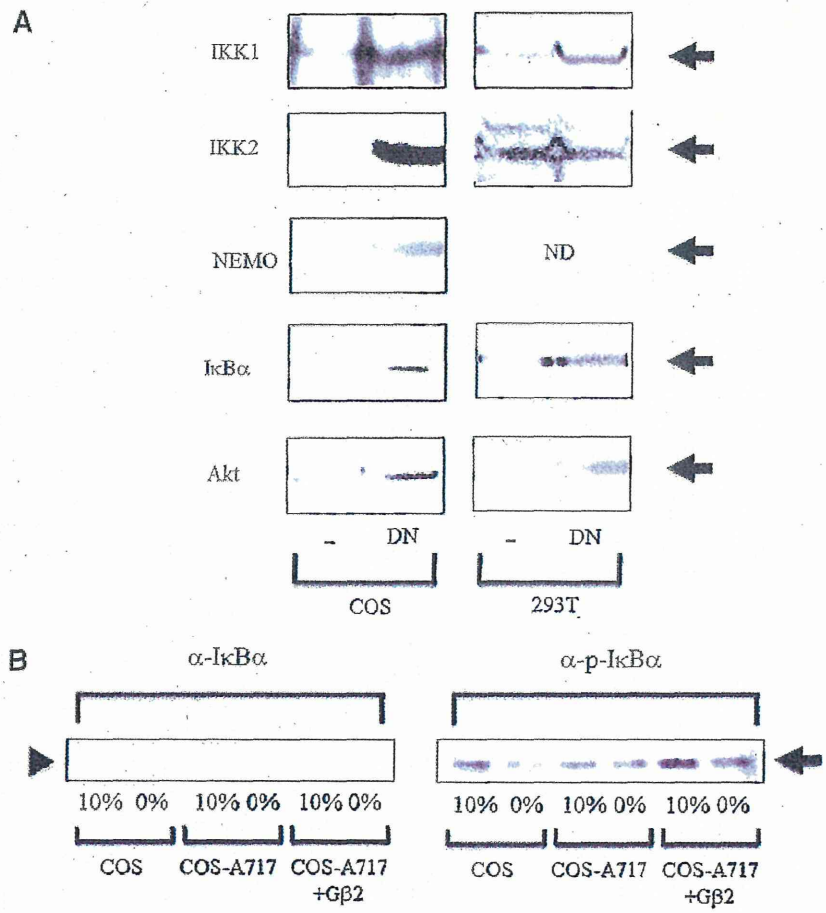

FIG. 5. (A) Expressions of the dominant negative and endogenous IKK1, IKK2, NEMO, IκBα, and Akt. COS cells were transfected with 1 μg of the mutant expressing plasmids of IKK1.DN, IKK2.DN, NEMO.DN, superrepressor of IκB (IκB-SR), and Akt.DN (refer to Table 1) in a six-well plate, and the cell lysates were prepared using 100 μL Glo lysis buffer (Promega) after 48h incubation. HEK293T cells were also transfected with the same plasmids, and prepared for Western blot. The description of antibodies is shown in Table 1. The *arrows* indicate the described proteins. N.D: not done. (B) COS, COS-A717, and COS-A717-Gβ2 cells were washed with PBS and incubated with (10%) without FBS (0%) for 24 h, and lysed with Glo lysis buffer. The positions of total IκBα, and phospho-IκBα were indicated with *arrowhead* and *arrow*, respectively.

dominant negative mutant is likely to be expressed enough to suppress its endogenous protein.To evaluate the phosphorylation and degradation of IkBα in COS, COSA717, and COSA717-Gβ2 cells by serum deprivation, we carried out Western blotting analysis using their specific antibodies. There were no significant changes in the phosphorylation of IκBα of COS, COSA717, and COSA717-Gβ2 cells by serum deprivation, using a phosphorylation-specific antibody (right panel of Fig. 5B). We could not assess the degradation of IκBα, because the anti-IκBα antibody was actually able to detect the human IκBα protein, but not simian COS IκBα, or because the IκBα expression in COS cell is too low to be detected by this antibody (Fig. 5A and left panel of Fig. 5B). The NF-κB activation by serum deprivation was dependent on IKK1, IKK2, NEMO, and IκBα, and this unique characteristic was not related to the IκBα phosphorylations at S32 and S36.

Because PI3K and Akt are upstream factors of IKKs in the NF-κB activation pathway (Ozes *et al.*, 1999; Romashkova and Makarov, 1999; Xie *et al.*, 2000), we examined whether the Gβ2-induced NF-κB activation occurs through PI3K and Akt activation. However, the PI3K inhibitor,Wortmannin, and a dominant negative mutant of Akt did not affect the Gβ2-induced NF-κB activation in COS-A717 cells (Fig. 4E, F). This result suggests that PI3K and Akt is not involved in the Gβ2-induced NF-κB activation.

Discussion

Many cell stresses activate NF-κB. We have shown here that serum starvation activates NF-κB signal, indicating that serum contains unknown inhibitor(s) of NF-κB signal. Cell stresses, such as radiation (Criswell *et al.*, 2003), oxidation (Marshall *et al.*, 2000), and UV (Kato *et al.*, 2003) positively control the NF-κB signaling. Interestingly, serum negatively regulates the NF-κB signaling, and starvation stress induces NF-κB activation by exclusion of the negative factor of serum.

Serum starvation activated NF-κB signaling in COS cells, but not in COS-A717 cells. The transfection of COS-A717 cells with Gβ2 partially restored the serum starvation-induced NF-κB activation. This result indicates that Gβ2 is required for the starvation-induced NF-κB activation, and the serum inhibitor suppresses the Gβ2-induced signaling pathway (Fig. 6).

Serum starvation of cells is frequently used in many biological experiments, including cell cycle synchronization and induction of apoptosis and autophagy. These biological events induced by starvation unexpectedly include the activation of Gβ2 and NF-κB signals. Therefore, these signaling might affect the synchronization of the cell cycle and the induction of apoptosis and authophagy by starvation, and scientists should consider the effects of the Gβ2 and NF-κB signals in the biological experiments using serum starvation.

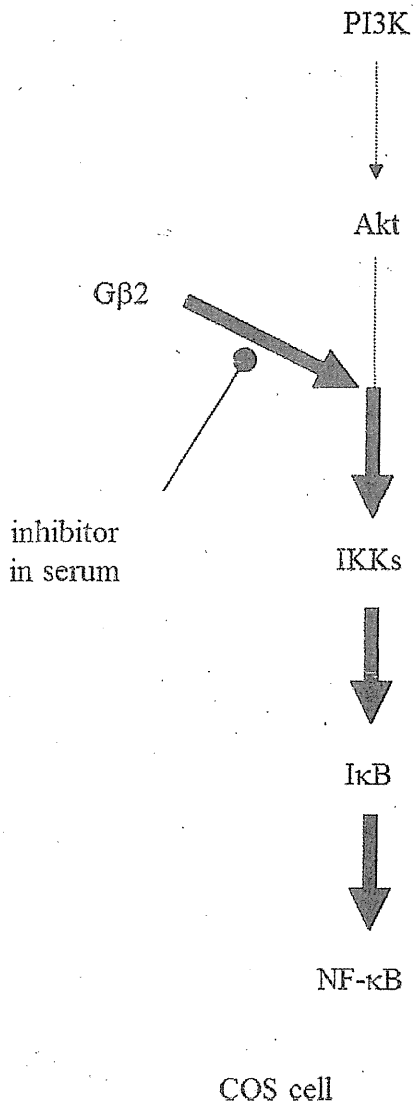

FIG. 6. Signaling pathway of NF-κB activation by Gβ2 or serum starvation.

We are trying to identify the serum inhibitor, and it will provide great impacts into many biological research fields.

NF-κB is constitutively activated in several transformed cell lines, suggesting that NF-κB signaling is involved in cellular transformation. However, the mechanism has not been elucidated yet. COS-A717 cells are mutant cells in which the basal NF-κB activity is much lower compared with the parental COS cells. Here, we showed that COS-A717 cells expressed a lower level of Gβ2 than COS cells, and the transfection of COS-A717 cells with Gβ2 restored the basal NF-κB activity, suggesting that the reduced expression level of Gβ2 is responsible for the defective NF-κB signaling in COS-A717 cells. Furthermore, the knockdown of Gβ2 expression by siRNA reduced the basal NF-κB activity not only in the COS cells, but also in the HT1080 cells, another transformed cell line with constitutively activated NF-κB signaling. These results indicate that Gβ2 is required for the constitutive activation of NF-κB in these transformed cells. This conclusion is strongly supported by previous reports showing that certain GPCR signals or the Gβ1γ2 complex activate NF-κB signaling (Xie *et al.*, 2000; Grabiner *et al.*, 2007; Sun *et al.*, 2009). Furthermore, the Tax oncoprotein of HTLV-1 activates NF-κB (Mori *et al.*, 1999; Gohda *et al.*, 2007) as well as the signals of CXCR4, a GPCR, by binding to the Gβ subunit (Twizere *et al.*, 2007), consistent with our conclusion. Although the Gβγ complex activates NF-κB through PI3K (Stephens *et al.*, 1994; Xie *et al.*, 2000), a PI3K inhibitor did not affect the Gβ2-induced NF-κB activation, suggesting that Gβ2 activates independently of PI3K in the NF-κB activation pathway (Fig. 6).

In summary, this study found that Gβ2-induced signaling activates NF-κB independently of PI3K and Akt in COS cells (Fig. 6). Unknown factor(s) present in serum inhibit the Gβ2-induced signaling. Therefore, serum starvation activates NF-κB by removing the serum inhibitor(s). The Gβ2-induced signaling is the target of the serum inhibitor, because exclusion of the serum inhibitor by starvation elevates NF-κB activity in Gβ2-expressing COS cells, but does not affect in Gβ2-defective COS-A717 cells.

Acknowledgments

We thank Dr. S. Yamaoka (Tokyo Medical and Dental University, Tokyo, Japan) for the plasmids expressing dominant negative forms of IKK1 (IKK1.DN), IKK2 (IKK2.DN), and NEMO (NEMO.DN), and Dr. V. Stambolic (Ontario Cancer Institute, Toronto, Canada) for the Akt dominant negative (Akt.DN) expression plasmid. This work was supported by Grants-in-Aid from the Ministry of Education, Culture, Sports, Science and Technology of Japan (22659092), and by the Global Center of Excellence Program at Nagasaki University (www.tm.nagasaki-u.ac.jp/gcoe).

Disclosure Statement

No competing financial interests exist.

References

Albert, P.R., and Robillard, L. (2002). G protein specificity: traffic direction required. Cell Signal **14**, 407–418.

Brown, K., Gerstberger, S., Carlson, L., Franzoso, G., and Siebenlist, U. (1995). Control of IκBα proteolysis by site-specific, signal-induced phosphorylation. Science **267**, 1485–1488.

Chen, Z., Hagler, J., Palombella, V.J., Melandri, F., Scherer, D., Ballard, D., and Maniatis, T. (1995). Signal-induced site-specific phosphorylation targets IκBα to the ubiquitin–proteasome pathway. Genes Dev **9**, 1586–1597.

Criswell, T., Leskov, K., Miyamoto, S., Luo, G., and Boothman, D.A. (2003). Transcription factors activated in mammalian cells after clinically relevant doses of ionizing radiation. Oncogene **22**, 5813–5827.

Gohda, J., Irisawa, M., Tanaka, Y., Sato, S., Ohtani, K., Fujisawa, J., and Inoue, J. (2007). HTLV-1 Tax-induced NF-κB activation is independent of lys-63-linked type polyubiquitination. Biochem Biophys Res Commun **357**, 225–230.

Grabiner, B.C., Blonska, M., Lin, P., You, Y., Wang, D., Sun, J., Darnay, B.G., Dong, C., and Lin, X. (2007). CARMA3 deficiency abrogates G protein-coupled receptor-induced NF-κB activation. Genes Dev **21**, 984–996.

Grimm, S., Bauer, M.K., Baeuerla, P.A., and Schulze-Osthoff, K. (1996). Bcl-2 down-regulates the activity of transcription factor NF-κB induced upon apoptosis. J Cell Biol **134**, 13–23.

Hironaka, N., Mochida, K., Mori, N., Maeda, M., Yamamoto, N., and Yamaoka, S. (2004). Tax-independent constitutive IkappaB kinase activation in adult T-cell leukemia cells. Neoplasia **6**, 266–278.

Hirt, B. (1967). Selective extraction of polyoma DNA from infected mouse cell cultures. J Mol Biol **26**, 365–369.

Jones, P.A., Laug, W.E., and Benedict, W.F. (1975). Fibrinolytic activity in a human fibrosarcoma cell line and evidence for the induction of plasminogen activator secretion during tumor formation. Cell **6**, 245–252.

Kato, T., Jr., Delhase, M., Hoffmann, A., and Karin, M. (2003). CK2 Is a C-Terminal IkappaB Kinase Responsible for NF-kappaB Activation during the UV Response. Mol Cell **12**, 829–839.

Kohno, T., Daa, T., Otani, H., Shimokawa, I., Yokoyama, S., and Matsuyama, T. (2008). Aberrant expression of BAFF receptor, a member of the tumor necrosis factor receptor family, in malignant cells of nonhematopoietic origins. Genes Cells **13**, 1061–1073.

Lilienbaum, A., and Israël, A. (2003). From calcium to NF-kappa B signaling pathways in neurons. Mol Cell Biol **23**, 2680–2698.

Lind, D.S., Hochwald, S.N., Malaty, J., Rekkas, S., Hebig, P., Mishra, G., Moldawer, L.L., Copeland, E.M. 3rd., and Mackay, S. (2001). Nuclear factor-kappa B is upregulated in colorectal cancer. Surgery **130**, 363–369.

Marshall, H.E., Merchant, K., and Stamler, J.S. (2000). Nitrosation and oxidation in the regulation of gene expression. FASEB J **14**, 1889–900.

Mori, N., Fujii, M., Ikeda, S., Yamada, Y., Tomonaga, M., Ballard, D.W., Yamamoto, N. (1999). Constitutive activation of NF-kappa B in primary adult T-cell leukemia cells. Blood **93**, 2360–2368.

Ozes, O.N., Mayo, L.D., Gustin, J.A., Pfeffer, S.R., Pfeffer, L.M., and Donner, D.B. (1999). NF-kappaB activation by tumor necrosis factor requires the Akt serine-threonine kinase. Nature **401**, 82–85.

Pagliari, L.J., Perlman, H., Liu, H., and Pope, R.M. (2000). Macrophages require constitutive NF-kappaB activation to maintain A1 expression and mitochondrial homeostasis. Mol Cell Biol **20**, 8855–8865.

Romashkova, J.A., and Makarov, S.S. (1999). NF-kappaB is a target of AKT in anti-apoptotic PDGF signaling. Nature **401**, 86–90.

Ryter, S.W., and Gomer, C.J. (1993). Nuclear factor kappa B-binding activity in mouse L1210 cells following photofrin II-mediated photosensitization. Photochem Photobiol **58**, 753–756.

Stephens, L., Smrcka, A., Cooke, F.T., Jackson, T.R., Sternweis, P.C., and Hawkins, P.T. (1994). A novel phosphoinositide 3 kinase activity in myeloid-derived cells is activated by G protein βγ subunits. Cell **77**, 83–93.

Sugita, S., Kohno, T., Yamamoto, K., Imaizumi, Y., Nakajima, H., Ishimaru, T., and Matsuyama, T. (2002). Induction of macrophage-inflammatory protein-3alpha gene expression by TNF-dependent NF-kappaB activation. J Immunol **168**, 5621–5628.

Sun, W., Li, H., Yu, Y., Fan, Y., Grabiner, B.C., Mao, R., Ge, N., Zhang, H., Fu, S., Lin, X., and Yang, J. (2009). MEKK3 is required for lysophosphatidic acid-induced NF-κB activation. Cell Signal **21**, 1488–1494.

Twizere, J.C., Springael, J.Y., Boxus, M., Burny, A., Dequiedt, F., Dewulf, J.F., Duchateau, J., Portetelle, D., Urbain, P., Van Lint, C., Green, P.L., Mahieux, R., Parmentier, M.,Willems, L., and Kettmann, R. (2007). Human T-cell leukemia virus type-1 Tax oncoprotein regulates G-protein signaling. Blood **109**, 1051–1060.

Wu, H.C., Huang, P.H., Chiu, C.Y., and Lin, C.T. (2001). G protein beta2 subunit antisense oligonucleotides inhibit cell proliferation and disorganize microtubule and mitotic spindle organization. J Cell Biochem **83**, 136–146.

Xie, P., Browning, D.D., Hay, N., Mackman, N., and Ye, R.D. (2000). Activation of NK-κB by bradykinin through a Gαq- and Gβγ-dependent pathway that involves phosphoinositide 3-kinase and Akt. J Biol Chem **275**, 24907–24914.

Yamada, Y. (1996). Features of the cytokines secreated by adult T-cell leukemia (ATL) cells. Leuk Lymphoma **21**, 443–447.

Yamaoka, S., Courtois, G., Bessia, C., Whiteside, S.T., Weil, R., Agou, F., Kirk, H.E., Kay, R.J., and Israel, A. (1998). Complementation cloning of NEMO, a component of the IkappaB kinase complex essential for NF-kappaB activation. Cell **93**, 1231–1240.

Zandi, E., Rothwarf, D.M., Delhase, M., Hayakawa, M., and Karin, M. (1997). The IκB kinase complex (IKK) contains two kinase subunits, IKKα and IKKβ, necessary for IκB phosphorylation and NF-κB activation. Cell **91**, 243–252.

Address correspondence to:
Hideki Hayashi, M.D., Ph.D.
Division of Cytokine Signaling
Department of Molecular Microbiology and Immunology
Graduate School of Biomedical Sciences
Nagasaki University
Nagasaki 852-8523
Japan

E-mail: hhayashi@nagasaki-u.ac.jp

Received for publication February 22, 2012; received in revised form July 6, 2012; accepted July 16, 2012.

ADORA2A polymorphism predisposes children to encephalopathy with febrile status epilepticus

Mayu Shinohara, Makiko Saitoh, Daisuke Nishizawa, et al.

Neurology 2013;80;1571; Published online before print March 27, 2013;
DOI 10.1212/WNL.0b013e31828f18d8

ADORA2A polymorphism predisposes children to encephalopathy with febrile status epilepticus

Mayu Shinohara, MS
Makiko Saitoh, MD
Daisuke Nishizawa, PhD
Kazutaka Ikeda, PhD
Shinichi Hirose, MD
Jun-ichi Takanashi, MD
Junko Takita, MD
Kenjiro Kikuchi, MD
Masaya Kubota, MD
Gaku Yamanaka, MD
Takashi Shiihara, MD
Akira Kumakura, MD
Masahiro Kikuchi, MD
Mitsuo Toyoshima, MD
Tomohide Goto, MD
Hideo Yamanouchi, MD
Masashi Mizuguchi, MD

Correspondence to
Dr. Saitoh:
makisaito-tky@umin.ac.jp

ABSTRACT

Objective: Acute encephalopathy with biphasic seizures and late reduced diffusion (AESD) is a childhood encephalopathy following severe febrile seizures, leaving neurologic sequelae in many patients. However, its pathogenesis remains unclear. In this study, we clarified that genetic variation in the adenosine A2A receptor (*ADORA2A*), whose activation is involved in excitotoxicity, may be a predisposing factor of AESD.

Methods: We analyzed 4 *ADORA2A* single nucleotide polymorphisms in 85 patients with AESD. The mRNA expression in brain samples, mRNA and protein expression in lymphoblasts, as well as the production of cyclic adenosine monophosphate (cAMP) by lymphoblasts in response to adenosine were compared among *ADORA2A* diplotypes.

Results: Four single nucleotide polymorphisms were completely linked, which resulted in 2 haplotypes, A and B. Haplotype A (C at rs2298383, T at rs5751876, deletion at rs35320474, and C at rs4822492) frequency in patients was significantly higher than in controls ($p = 0.005$). Homozygous haplotype A (AA diplotype) had a higher risk of developing AESD (odds ratio 2.32, 95% confidence interval 1.32–4.08; $p = 0.003$) via a recessive model. mRNA expression was significantly higher in AA than AB and BB diplotypes, both in the brain ($p = 0.003$ and 0.002, respectively) and lymphoblasts ($p = 0.035$ and 0.003, respectively). In lymphoblasts, ADORA2A protein expression ($p = 0.024$), as well as cellular cAMP production ($p = 0.0006$), was significantly higher in AA than BB diplotype.

Conclusions: AA diplotype of *ADORA2A* is associated with AESD and may alter the intracellular adenosine/cAMP cascade, thereby promoting seizures and excitotoxic brain damage in patients.

***Neurology*® 2013;80:1571–1576**

GLOSSARY

ADORA1 = adenosine A1 receptor; **ADORA2A** = adenosine A2A receptor; **AEIMSE** = acute encephalopathy with inflammation-mediated status epilepticus; **AESD** = acute encephalopathy with biphasic seizures and late reduced diffusion; **cAMP** = cyclic adenosine monophosphate; **CI** = confidence interval; **CPT2** = carnitine palmitoyltransferase II; **G6PDH** = glucose-6-phosphate dehydrogenase; **OR** = odds ratio; **SMRI** = Stanley Medical Research Institute; **SNP** = single nucleotide polymorphism.

During the course of acute febrile diseases, such as influenza and exanthema subitum, some children develop repetitive or prolonged seizures, followed by sustained impairment of consciousness. These conditions are collectively termed acute encephalopathy with inflammation-mediated status epilepticus (AEIMSE).[1] Among AEIMSE, acute encephalopathy with biphasic seizures and late reduced diffusion (AESD)[2] is the most common in Japan, affecting hundreds of children every year.[3] Hemiconvulsion-hemiplegia syndrome, a condition encountered worldwide, often occurs during an infectious disease, and is regarded as a subgroup of AESD.[4] AESD typically shows a biphasic clinical course, consisting of a prolonged febrile seizure

Supplemental data at www.neurology.org

From the Department of Developmental Medical Sciences (M. Shinohara, M. Saitoh, M.M.), Graduate School of Medicine, the University of Tokyo; Addictive Substance Project (D.N., K.I.), Tokyo Metropolitan Institute of Medical Sciences; Department of Pediatrics (S.H.), Fukuoka University; Department of Pediatrics (J.-i.T.), Kameda Medical Center; Department of Cell Therapy and Transplantation Medicine (J.T.), the University of Tokyo; Department of Pediatrics (K.K.), Saitama Medical Children's Hospital; Department of Neurology (M. Kubota), National Center for Child Health and Development; Department of Pediatrics (G.Y.), Tokyo Medical University; Department of Pediatrics (T.S.), Gunma Children's Medical Center; Department of Pediatrics (A.K.), Kitano Hospital; Department of Pediatrics (M. Kikuchi), Hitachi General Hospital; Department of Pediatrics (M.T.), Kagoshima University; Department of Pediatrics (T.G.), Tokyo Metropolitan Children's Medical Center; and Department of Pediatrics (H.Y.), Saitama Medical University, Japan.

Go to Neurology.org for full disclosures. Funding information and disclosures deemed relevant by the authors, if any, are provided at the end of the article.

on the first day and a cluster of complex partial seizures several days later (late seizure), each followed by postictal coma. Cranial MRI reveals high signal intensity lesions in the cerebral subcortical white matter on diffusion-weighted images, which appear around the occurrence of late seizure (figure 1).[5,6] Excitotoxicity is considered to be the main pathologic mechanism of AESD.[2,4] The genetic background of AESD remains to be elucidated. Recently, polymorphism of a gene encoding a mitochondrial enzyme, carnitine palmitoyltransferase II (*CPT2*), was identified as a genetic predisposition for AESD[7]; however, some patients with AESD have no such polymorphism, suggesting the involvement of genes other than *CPT2*.

We hypothesized that the adenosine-mediated signal pathway is altered in AESD because theophylline, a nonselective adenosine receptor antagonist, aggravates AESD.[4] To test this hypothesis, we studied the haplotype frequency of 4 single nucleotide polymorphisms (SNPs) located in the linkage disequilibrium block of the adenosine A2A receptor (*ADORA2A*) gene, and then examined the effects of *ADORA2A* diplotypes on their mRNA and protein expression, and those on cyclic adenosine monophosphate (cAMP) production in response to adenosine.

METHODS

Subjects. We recruited patients with AESD from hospitals in Japan during 2008–2011 based on the diagnostic criteria.[3] Eighty-five Japanese patients, 39 male and 46 female aged from 6 months to 10 years and 3 months (median, 1 year and 10 months), participated in this study. Detailed clinical data are shown in table e-1 on the *Neurology*® Web site at www.neurology.org. All patients had their first convulsion, mostly status epilepticus, within 24 hours from the onset of fever, followed by impairment of consciousness that improved on the second day in most cases. On the fourth to sixth day of illness, there was a recurrence of convulsions or a cluster of partial seizures, followed again by impairment of consciousness. Cranial MRI was normal on the first to second day of illness, but showed high signal intensity lesions in the cerebral subcortical white matter on the third to ninth day (figure 1). Pathogens of antecedent infections included human herpesvirus 6 (28 cases), influenza virus (5 cases), respiratory syncytial virus, rotavirus, adenovirus, mumps virus, and *Mycoplasma pneumoniae*.

Figure 1 Typical MRI findings of a patient with acute encephalopathy with biphasic seizures and late reduced diffusion

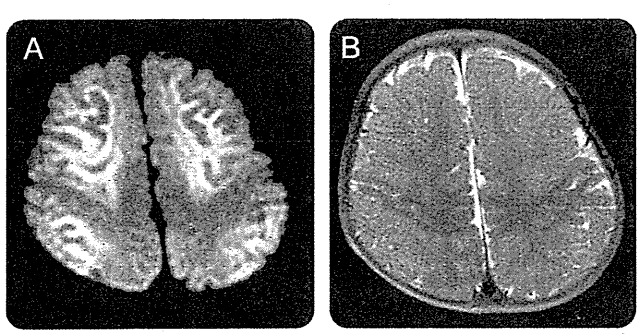

Magnetic resonance study of a 1-year-old boy on day 8 demonstrated lesions in the subcortical white matter that showed high signal intensity on diffusion-weighted (A) and T2-weighted (B) images. The lesions were prominent along the U-fibers with sparing of the peri-Rolandic region.

Standard protocol approvals, registrations, and patient consents. The procedures in this study were approved by the University of Tokyo Ethics Committee. Written informed consent was obtained from all guardians of participants in the study.

Controls. We analyzed the *ADORA2A* genotypes of control subjects, consisting of 100 healthy Japanese adults, 50 men and 50 women, 20 to 69 years of age, using DNA extracted from Pharma SNP Consortium B cell lines obtained from the Human Science Research Resources Bank (Osaka, Japan). We searched the dbSNP database (http://www.ncbi.nlm.nih.gov/projects/SNP/) in the National Center for Biotechnology Information for the variation frequencies of *ADORA2A* SNPs and combined the data of 100 controls from the Pharma SNP Consortium and those of 84 Japanese in the National Center for Biotechnology Information dbSNP database.

Brain samples. To examine *ADORA2A* gene expression levels in the brain, 100 human brain DNA and RNA samples were obtained from Stanley Medical Research Institute (SMRI) (Bethesda, MD). DNA and RNA were extracted from the occipital and anterior cingulate cortex, respectively. In this experiment, the ethnic background was Caucasian in the vast majority (at least 98 samples).

Lymphoblasts. For expression studies and functional assays, we used 15 lymphoblast cell lines from control Japanese adults, obtained from control subjects at the University of Tokyo Hospital.

Procedures. Peripheral blood samples were collected from the patients. Genomic DNA was extracted from the blood using standard protocols. All 5 exons of *ADORA2A* were PCR amplified with flanking intronic primers and standard PCR conditions (primer sequences are described in table e-2). PCR products of *ADORA2A* were sequenced on a 310 Genetic Analyzer, 3100 Genetic Analyzer, or 3130xl Genetic Analyzer (Life Technologies, Carlsbad, CA). To identify rs5751876 and rs2298383 SNPs, the PCR–restriction fragment length polymorphism method was adopted.[8] For quantitative PCR, total RNA was isolated from control lymphoblasts using TRIzol reagent (Life Technologies) according to the manufacturer's protocol. Total RNA was reversely transcribed to cDNA by a Ready-To-Go You-Prime First-Stand Beads cDNA synthesis kit (GE Healthcare, Uppsala, Sweden) according to the manufacturer's protocol. Random Primer (Takara Bio, Otsu, Japan) was used. Gene expression was evaluated by the relative Quantification ABI PRISM 7000 Sequence Detection System (Life Technologies) with FastStart Universal SYBR Green Master [ROX] (Roche, Basel, Switzerland) reagent. The relative *ADORA2A* mRNA expression level was calculated using glucose-6-phosphate dehydrogenase (G6PDH) as the internal standard. Primer sequences of real-time PCR for *ADORA2A* and *G6PDH* are described in table e-3. Each value is shown as the mean value of 2 independent experiments in triplicate. For SMRI brain samples, genotyping and the gene expression study of *ADORA2A* were performed by the same methods as for AESD patient samples. Western blotting

of the cell lysate from control lymphoblasts was performed by the standard protocol using a rabbit polyclonal antibody to human ADORA2A (Abcam, Cambridge, UK) at a dilution of 1:500. The relative ADORA2A protein expression level was calculated using β-actin as the internal standard. Each value is shown as the mean value of 3 independent experiments in duplicate. The cAMP concentration in lymphoblasts was measured after stimulation by adenosine (10 nM) and 8-cyclopentyl-1,3-dipropylxanthine (10 nM), a selective adenosine A1 receptor (ADORA1) antagonist, using the cAMP-Screen Direct System (Life Technologies) according to the manufacturer's protocol. Cellular cAMP levels were determined using SpectraMax Pro 5.3 software (Molecular Devices, Sunnyvale, CA). Each value is shown as the mean value of 2 independent experiments in triplicate.

Statistical analysis. Differences in the demographic characteristics of the genotypes between patients (85 cases) and controls were assessed by Pearson χ^2 test and Fisher exact test for categorical data. Goodness-of-fit to the Hardy-Weinberg equilibrium and differences in genotype and allele frequencies between AESD and control groups were examined by χ^2 analysis. Significant differences were defined as $p < 0.05$ in conditional analysis. We estimated the odds ratio (OR) together with the 95% confidence interval (CI) for each allele haplotype frequency with AESD using Microsoft Office Excel 2010. Patients with AESD were compared with the controls under dominant, recessive, and additive models using a likelihood ratio χ^2 test. These genetic models were also assessed using the Cochran-Armitage test for trend. The differences in mRNA and protein expression levels and cellular cAMP accumulation, expressed as the mean ± SEM, were calculated using analysis of variance followed by the Tukey-Kramer test in the case of multiple comparisons. $p < 0.05$ was considered a significant difference.

RESULTS

***ADORA2A* haplotype frequency.** First, we analyzed the entire coding region of *ADORA2A* in patients with AESD and found no mutations. Second, we analyzed genetic variations of *ADORA2A* in patients with AESD and control subjects. Distribution of the *ADORA2A* polymorphisms in both AESD and controls met the Hardy-Weinberg equilibrium ($p = 0.15$ and 0.86, respectively). Four SNPs (figure e-1) in this gene, rs2298383, rs5751876, rs35320474, and rs4822492, had previously been reported to show complete linkage disequilibrium in 84 Japanese (human HapMap project, http://Apr2011.archive.ensemble.org). The present study also supported their complete linkage in both 85 AESD cases and 100 controls. Thus, there were only 2 haplotypes, haplotype A (C at rs2298383, T at rs5751876, deletion at rs35320474, and C at rs4822492) and haplotype B (T at rs2298383, C at rs5751876, T at rs35320474, and G at rs4822492). Table 1 shows haplotype frequency for the *ADORA2A* SNPs in AESD and control groups. Haplotype A was significantly more frequent in AESD than in controls ($p = 0.005$). The frequency of homozygous haplotype A (AA diplotype) in AESD and controls was 37.6% and 20.6%, respectively. There was a significant association between AA diplotype and increased risk of developing AESD for recessive model comparison (OR 2.32, 95% CI 1.32–4.08; $p = 0.003$) and additive model comparison (OR 2.62, 95% CI 1.29–5.32; $p = 0.007$), but not for the dominant model comparison (OR 1.63, 95% CI 0.89–2.99; $p = 0.142$) (table 2). The most significant p value was obtained under the recessive model using χ^2 test, as well as Cochran-Armitage test for trend.

***ADORA2A* mRNA expression in the brain.** Second, to evaluate the association of *ADORA2A* diplotypes with gene expression in the CNS tissue, we measured the amount of *ADORA2A* mRNA in SMRI samples after genotyping. Because the 4 SNPs were completely linked in 95 of 100 subjects (diplotype AA, 19 subjects; AB, 38 subjects; and BB, 38 subjects), we used these 95 samples. The relative expression level of *ADORA2A* mRNA (mean ± SEM) in AA, AB, and BB diplotypes was 0.246 ± 0.025, 0.179 ± 0.009, and 0.177 ± 0.009, respectively (figure 2). The expression level was 1.4-fold higher in the AA diplotype than in AB and BB, showing a significant difference ($p = 0.003$ and 0.002, respectively).

***ADORA2A* mRNA and protein expression and production of cAMP in lymphoblasts.** ADORA2A is highly expressed in brain, heart, kidney, and lymphocytes.[9,10] Because protein samples from the brain were unavailable, we used lymphoblast cell lines to determine the effect of *ADORA2A* diplotypes on ADORA2A protein expression. We again showed that the expression of *ADORA2A* mRNA in lymphoblasts with AA diplotype was higher than in those with AB and BB (figure 3A,

Table 1 Comparison of *ADORA2A* haplotype frequency between patients with AESD and controls[a]

	Genotype				AESD		Control[b]		Test for allele haplotype frequency
Haplotype	rs2298383	rs5751876	rs35320474	rs4822492	n	%	n	%	OR (95% CI)
A	C	T	del	C	99	58.2	166	45.1	1.70 (1.17–2.45)
B	T	C	T	G	71	41.8	202	54.9	
Total					170		368		

Abbreviations: AESD = acute encephalopathy with biphasic seizures and late reduced diffusion; CI = confidence interval; OR = odds ratio.
[a] Difference in haplotype frequency between patients and controls was statistically significant ($p = 0.005$).
[b] Data of Pharma SNP Consortium B cell samples and those of HapMap (JPT) were combined.

Table 2 Comparison of *ADORA2A* diplotype distribution between patients with AESD and controls

Diplotype	AESD (n = 85), n (%)	Control (n = 184),[a] n (%)	OR (95% CI), *p* value	
AA	32 (37.6)	38 (20.6)	2.62 (1.29–5.32), 0.007	
AB	35 (41.2)	90 (49.0)	1.21 (0.62–2.34), 0.612	
BB	18 (21.2)	56 (30.4)	1.00 (reference)	
Genetic model				*p* Value for trend test
Recessive	AA vs AB + BB		2.32 (1.32–4.08), 0.003	0.003
Dominant	AA + AB vs BB		1.63 (0.89–2.99), 0.142	0.114
Additive	AA vs BB		2.62 (1.29–5.32), 0.007	0.006

Abbreviations: AESD = acute encephalopathy with biphasic seizures and late reduced diffusion; CI = confidence interval; OR = odds ratio.
[a] Data of Pharma SNP Consortium B cell samples and those of HapMap (JPT) were combined.

$p = 0.035$ and 0.003, respectively). By Western blotting, the relative ADORA2A protein level (mean ± SEM) was evaluated as 0.611 ± 0.045, 0.439 ± 0.022, and 0.443 ± 0.044 for AA, AB, and BB, respectively (figure 3B). The protein expression was significantly higher in AA diplotype than in AB and BB ($p = 0.021$ and 0.024, respectively). Next, to elucidate the difference of intracellular signal transduction among 3 *ADORA2A* diplotypes, cAMP assay was performed. The cellular cAMP accumulation level (mean ± SEM) for AA, AB, and BB diplotypes was 2.016 ± 0.207, 1.421 ± 0.186, and 0.953 ± 0.118 pmol, respectively (figure 3C). As the number of haplotype A alleles increased, so did the adenosine-stimulated cAMP production. The cAMP level was significantly higher in the AA diplotype than in BB ($p = 0.0006$).

DISCUSSION Previous studies have shown the complex roles of adenosine in the brain, deriving from the diversity of receptor subtypes. In the CNS, ADORA2A competes with ADORA1 in various neural functions. For synaptic transmission, ADORA2A enhances excitatory neurotransmitter release, whereas ADORA1 exerts an inhibitory effect.[11] The role of adenosine as an endogenous anticonvulsant is mediated via ADORA1.[12] Inhibition of ADORA1 function has been shown to cause status epilepticus.[13] In a rat model of seizure kindling, ADORA1 in the hippocampal CA1 region reduces seizures, whereas ADORA2A promotes them.[14] *Adora2a* knockout mice show a reduction of ethanol-induced seizures,[15] whereas activation of ADORA2A renders rat pups susceptible to hyperthermia-induced seizures.[16] Despite these findings, the association of *ADORA2A* variations with a seizure disorder has never been reported. They are known to be associated with anxiety induced by caffeine, an antagonist of ADORA1 and ADORA2A.[17–19]

Figure 2 *ADORA2A* mRNA expression in the brain with different *ADORA2A* diplotypes

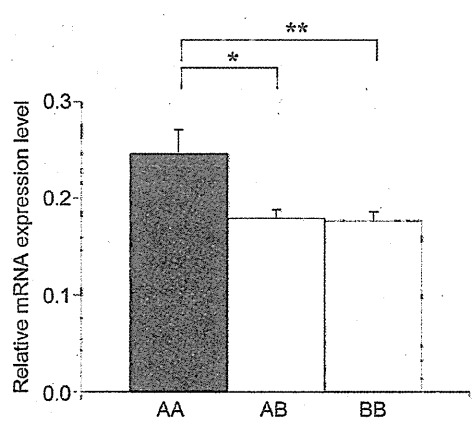

Relative *ADORA2A* mRNA expression level (*ADORA2A*/*G6PDH*) in the brain was higher in the AA diplotype (n = 19) than in AB (n = 38, *$p = 0.003$) and BB (n = 38, **$p = 0.002$).

The present study showed for the first time the association between an *ADORA2A* genetic variant and AESD, a typical syndrome of AEIMSE during early childhood. The results suggest that *ADORA2A* AA diplotype predisposes children to AESD by altering the intracellular adenosine/cAMP signal cascade.

We demonstrated that the frequency of *ADORA2A* AA diplotype was significantly higher in patients with AESD than in controls (table 2). These data show an apparent association between AA diplotype and AESD, although whether the recessive or additive model most accurately describes this association is unclear at this time. Haplotype A consists of 4 SNPs, rs2298383, rs5751876, rs35320474, and rs4822492, which show complete linkage disequilibrium with one another in Japanese. The rs2298383 SNP is located in a potential promoter region upstream of the recently identified exon variant,[8] with a regulatory element predicted from alignment of human and other mammalian genes.[20] Further evidence of its importance in gene expression regulation is provided by in silico analyses,[21] which indicated the position

Figure 3 *ADORA2A* mRNA expression, ADORA2A protein expression, and cAMP production in lymphoblasts with different *ADORA2A* diplotypes

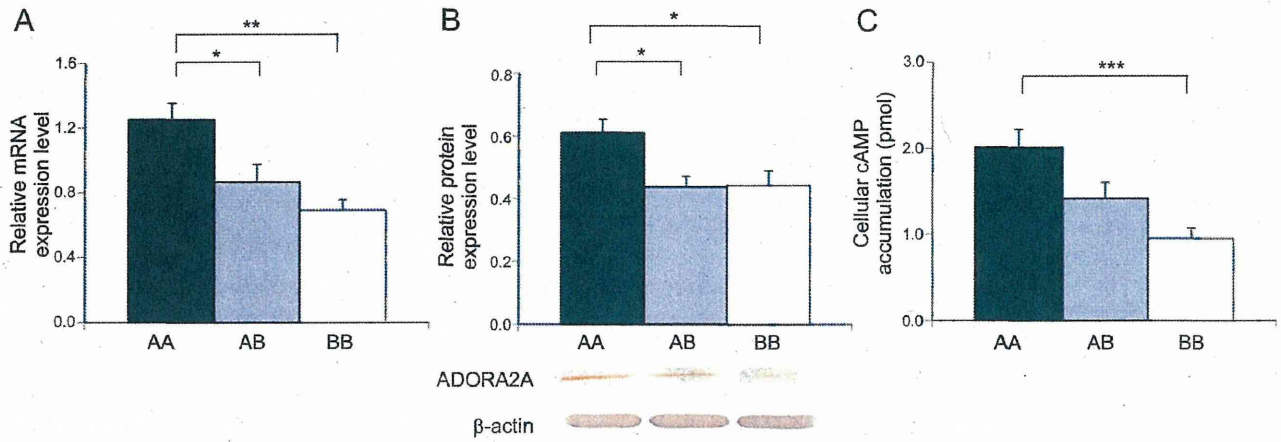

(A) Relative *ADORA2A* mRNA expression level (*ADORA2A*/*G6PDH*) is higher in AA diplotype than in AB (*$p = 0.035$) and BB (**$p = 0.003$) (n = 5 for each diplotype). (B) Relative ADORA2A protein expression level (ADORA2A/β-actin) was higher in AA than in AB (*$p = 0.021$) and BB (*$p = 0.024$) (n = 5 for each diplotype). Lower panel shows results of a representative Western blot, showing increasing band intensity with the number of haplotype A. (C) Cyclic adenosine monophosphate (cAMP) production in response to adenosine was higher in diplotype AA than in BB (***$p = 0.0006$) (n = 5 for each diplotype).

of rs2298383 SNP within a triplex-forming oligonucleotide target sequence. The 35320474 SNP is located in the 3′ untranslated region including U-rich motifs. U-rich motifs are conserved across species and provide active sites for interaction with RNA-binding proteins. Thus, any of these SNPs may possibly alter the expression level of mRNA.

In fact, we found that the *ADORA2A* AA diplotype causes a high expression of *ADORA2A* mRNA in the brain and lymphoblasts, and a high expression of ADORA2A protein in lymphoblasts. Given its excitatory function, increased expression of ADORA2A may cause a functional imbalance between ADORA1 and ADORA2A, resulting in hyperexcitation of cerebral neurons.

In the present study, cellular cAMP accumulation in response to adenosine was high in lymphoblasts with *ADORA2A* AA diplotype. ADORA2A, together with coupled Gs proteins, activates adenylate cyclase and increases the cellular cAMP level. In this study, we observed high cellular cAMP in the AA diplotype, which supports our hypothesis that the signal cascade downstream of ADORA2A is excessively activated in AESD. cAMP promotes protein kinase A, which in turn enhances Ca^{2+} influx through the L-type Ca^{2+} channel in the basal ganglia, hippocampus, and striatum. Ca^{2+} then enhances glutamate efflux from the endoplasmic reticulum to the extracellular space, leading to excitotoxicity.[22–25] An increase of extracellular glutamate in the brain lesion of AESD has recently been demonstrated by magnetic resonance spectrometry.[5]

Involvement of ADORA2A in the pathogenesis of AESD may have therapeutic implications. Experimental studies have previously shown that an ADORA2A antagonist, but not an ADORA1 agonist, can terminate or suppress seizures.[26,27] Pharmacologic blockade or genetic disruption of ADORA2A may protect neurons from seizures by reducing glutamate release and excitotoxicity.[27] Thus, ADORA2A antagonists are promising candidate drugs to ameliorate seizure-induced brain damage. Because this study showed alteration of the ADORA2A signal cascade in AESD, these drugs may also be particularly useful in the treatment of AESD. However, our data showed that 20% of patients with AESD have the BB diplotype, suggesting the involvement of factors other than *ADORA2A* in the etiology of AESD.

In conclusion, the present study demonstrated that polymorphisms of the *ADORA2A*, or AA diplotype, are risk factors of AESD, an acute encephalopathy with febrile status epilepticus. This diplotype showed a high ADORA2A expression level and high cAMP accumulation in response to adenosine, suggesting the involvement of the adenosine/cAMP signal cascade in the pathogenesis of AESD. Pharmacologic intervention in this pathway may improve the treatment of children with this devastating encephalopathy.

AUTHOR CONTRIBUTIONS

M. Shinohara contributed to analysis and interpretation of the data. M. Saitoh contributed to design and conceptualization of the study, interpretation of the data, draft and revision of the manuscript for intellectual content. D. Nishizawa contributed to analysis and interpretation of the data. K. Ikeda contributed to design and conceptualization of the study, interpretation of the data, draft and revision of the manuscript for intellectual content. S. Hirose contributed to analysis and interpretation of the data. J. Takanashi, J. Takita, K. Kikuchi, M. Kubota, G. Yamanaka, T. Shiihara, A. Kumakura, M. Kikuchi, M. Toyoshima, T. Goto, and H. Yamanouchi contributed to interpretation of the data. M. Mizuguchi